Future snow projections in a small basin of the Western Himalaya

Santosh Nepal [a,*], Kabi Raj Khatiwada [a], Saurav Pradhananga [a], Sven Kralisch [b,c], Denis Samyn [a], Mohammad Tayib Bromand [d], Najeebullah Jamal [d], Milad Dildar [a], Fazlullah Durrani [d], Farangis Rassouly [d], Fayezurahman Azizi [d], Wahidullah Salehi [d], Rohullah Malikzooi [e], Peter Krause [f], Sujan Koirala [g], Pierre Chevallier [h]

[a] International Centre for Integrated Mountain Development, Kathmandu, Nepal
[b] Department of Geoinformation Science, Friedrich Schiller University Jena, Jena, Germany
[c] Institute of Data Science, German Aerospace Center (DLR), Jena, Germany
[d] National Water Affairs Regulation Authority (NWARA), Afghanistan
[e] Kabul Polytechnic University (KPU), Kabul, Afghanistan
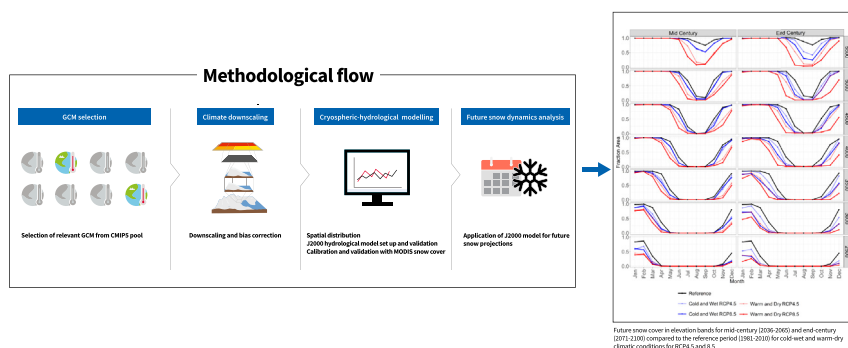[f] Thuringian State Agency for Environment, Mining and Nature Conservation, Jena, Germany
[g] Department of Biogeochemical Integration, Max Planck Institute for Biogeochemistry, Jena, Germany
[h] HydroSciences Laboratory (CNRS, IRD, University of Montpellier), Montpellier, France

HIGHLIGHTS

- We used an integrated methodology to select reliable global climate models and simulate snow cover dynamics.
- Snow cover in the autumn and spring seasons is projected to reduce by as much as 25% by the end of the century.
- Snowmelt is likely to increase in winter and spring and decrease in summer in the Panjshir catchment.
- The reduced snow cover in the future might impact melt runoff-dependent sectors in the Western Himalaya.

GRAPHICAL ABSTRACT

Future snow cover in elevation bands for mid-century (2036-2065) and end-century (2071-2100) compared to the reference period (1981-2010) for cold-wet and warm-dry climatic conditions for RCP4.5 and 8.5

ARTICLE INFO

ABSTRACT

Snow is a crucial component of the hydrological cycle in the Western Himalaya. Water from snowmelt is used in various sectors in downstream regions, thus playing a critical role in securing the livelihoods of millions of people. In this study, we investigated the future evolution of snow cover and snowmelt in the Panjshir catchment of Afghanistan, a sub-basin of the Indus, in the Western Himalaya. We applied a three-step approach to select a few global climate model (GCM) simulations from CMIP5 climate datasets for RCP4.5 and RCP8.5, which showed reasonable performance with ERA5-Land dataset for the chosen historical period (1981–2010). The selected model simulations were then segregated into two groups: those projecting a cold-wet climate and those projecting a warm-dry climate by the end of the 21st century (2071–2100). These GCMs were downscaled to a higher resolution using empirical statistical downscaling. To simulate the snow processes, we used the distributed cryospheric-hydrological J2000 model. The results indicate that the model captures well the snow cover dynamics for the historical period when compared with the daily MODIS-derived snow cover. The J2000 model was then forced by climate projections from the selected GCMs to quantify future changes in snow cover area, snow storage and snowmelt. While a 10–18% reduction in annual snow cover area is projected in the cold-wet models, a 22–36% reduction is projected in the warm-dry models. Similarly, the snow cover area is projected to decrease in all elevation bands under climate change. At the seasonal scale, across all models and scenarios, the snow cover

* Corresponding author.
 E-mail address: Santosh.Nepal@icimod.org (S. Nepal).

Panjshir
Afghanistan

in the autumn and spring seasons are projected to reduce by as much as 25%, with an increase in winter and spring snowmelt and a decrease in summer snowmelt. The projected changes in the seasonal availability of snowmelt-driven water resources are likely to have direct implications for water-dependent sectors in the region and call for a better understanding of water usage and future adaptation practices.

1. Introduction

Snowfall, snow storage and snowmelt are important processes of the mountain cryosphere. Snow storage, in different forms, provides a natural water reservoir in high altitude areas and creates various scales of time lags (from daily to multi-year levels) in supplying freshwater for downstream uses (Armstrong et al., 2019; Jeelani et al., 2012). Snowmelt provides freshwater to up to 17% of the world's population (Barnett et al., 2005; Bormann et al., 2018). This unique characteristic of the mountains, in the form of water storage, creates an important linkage between the upstream water supply and the various uses of water in downstream regions (Nepal et al., 2018; Scott et al., 2019; Viviroli et al., 2020).

Mountain snow cover is characterised by a strong interannual and decadal variability (Bolch et al., 2019; Hock et al., 2019). In the Hindu Kush Himalaya (HKH) region, a substantial proportion of the annual precipitation is available in the form of snow in areas above 3000 m above sea level (a.s.l.) (Gurung et al., 2011; Kripalani et al., 2007; Ménégoz et al., 2013). Snow plays a key role in the 10 major river systems originating from the HKH region (Bolch et al., 2019; Hock et al., 2019; Nie et al., 2021), where roughly 240 million people live, with an additional 1.65 billion people living in the related river basins (Sharma et al., 2019).

In the Indus basin, 60% of the total irrigation water withdrawal in the spring season originates from mountain snow and glacier melt, and that contributes ~11% to the total crop production (Biemans et al., 2019). The large contribution of snowmelt underpins the socioeconomic significance of snowmelt, and thus makes it one of the most critical water towers of the world that supports dense population and intensive irrigation (Immerzeel et al., 2020). Furthermore, in the context of projected climate change, the Indus basin is very vulnerable to adverse impacts on overall environmental conditions (Dahri et al., 2021). Therefore, a better understanding of the evolution of future snow-related variables is socio-economically crucial for communities and water-dependent sectors in the Western Himalaya region.

Climate change alters the key variables driving the onset and development of snow cover, manifesting itself through a decline in lower elevation snow cover throughout the globe (Bormann et al., 2018; Hock et al., 2019). The patterns of snow cover vary across the Indus, Ganges, and Brahmaputra river basins due to spatio-temporally heterogeneous responses to climate. Different evaluations of the changes in patterns predict either no significant change in the snow cover (e.g., Singh et al., 2014) or large changes in specific regions of the HKH. In the Nepal Himalaya, Maskey et al. (2011) reported both increasing and decreasing snow cover trends depending on the months considered. In the Hunza catchment (part of the Indus basin) of Pakistan, on the other hand, Tahir et al. (2011) showed a slight increase in the cryosphere area (glacier and snow cover) in the recent decades that was attributed to an increase in winter precipitation. Chevallier et al. (2014), however, projected a gradual loss of the snowmelt influence on the river flow regime in Pamir Alay, Central Asia. Similarly, Kripalani et al. (2003) reported both a declining spring snow cover area and faster snowmelt in the western Himalaya region. A study by Zaman and Khan (2020) showed no clear trend between the years 2001 and 2016, with a slightly increasing trend between 2001 and 2007 followed by a decreasing trend between 2012 and 2016. According to Hock et al. (2019), most of the changes in snow cover, in general, can be attributed to a snowmelt increase due to increased air temperature, which, at lower elevations, translates into a shift from solid to liquid precipitation (i.e., rain).

It is widely anticipated that climate change will lead to reduced snow cover and snow volume, mainly because of an increase in temperature in the Himalaya region (Bolch et al., 2012). Viste and Sorteberg (2015) estimated a decrease of 30–50% in the annual snowfall under RCP8.5 by the end of the century in the Indus basin. Over the same time period, in the Himalaya region, Terzago et al. (2014b) estimated a decrease in snow depth between 17% to 39% (compared to the historical period [1980–2005]) under the RCP4.5 and RCP8.5 scenarios, respectively. The snow line is also projected to recede by 400 to 900 m in the Himalaya region under the RCP8.5 scenario (Viste and Sorteberg, 2015). Azizi and Asaoka (2020) reported a decrease in seasonal snow cover area under climate change in the Panjshir catchment. Most global climate models agree on the increasing temperature trend in the HKH region, including elevation-dependent warming (Bolch et al., 2012; Kraaijenbrink et al., 2017). In various lower elevations regions, including in the Himalaya, the snow depth (or mass) is projected to decline by 25% on average (ranging from 10% to 40%) between the recent past (1986–2005) and the near future (2031–2050) (Hock et al., 2019). Similar changes in snow under climate change have also been reported in other global mountain ranges – e.g., a reduction in future snow cover in the European alps (Marty et al., 2017), a reduction in dry snowpack and increase in wet snowpack in the French Alps (Castebrunet et al., 2014), and a decrease in dry season snow cover at the rate of 12% per decade in the Andes (Cordero et al., 2019).

In the mountainous and immediate downstream areas of the western Himalaya, many sectors such as agriculture, hydropower, households and irrigation depend on water from snowfall, and melt runoff. Thus, changes in snow dynamics can adversely affect diverse environmental and community sectors, such as river hydrology (Gaddam et al., 2018; Jeelani et al., 2012), water availability (Barnett et al., 2005), agriculture, pasture and ecosystem integrity (Gentle and Maraseni, 2012; Ingty, 2017; Qin et al., 2006). Therefore, understanding and quantifying the impact of climate change on future snow dynamics is paramount.

While previous studies have evaluated the impact of climate change on snow in the HKH region, different snow-related variables such as for snowfall (Viste and Sorteberg, 2015), snow depth (Terzago et al., 2014a), snow cover and snowmelt (Azizi and Asaoka, 2020) have been assessed independently. Analysis of the snow cover changes for different elevation zones is also missing in the case of Western Himalaya. An integrated assessment of climate change impacts on snowfall, snow cover, snow storage and snowmelt is necessary to understand the overall changes in snow dynamics and the driving mechanisms and reasons behind them. Such assessments, despite being critical for the socio-economic well-being of the downstream population, are scarce for the Western Himalaya.

Furthermore, previous studies in the HKH are mostly focused on larger basins (i.e., with an area greater than 2500 km²), even though the changes in snow dynamics are more relevant at smaller scales, especially with regards to process formulations in models and implications on meltwater uses at the local scale. Recently, changes in snow were evaluated for the Everest region in the Central Himalaya (Bouchard et al., 2019; Mimeau et al., 2019), but the changes in the Western Himalaya – with its pronounced climate with lower precipitation and temperature – are still unclear. This study aims to fill that gap by

providing an integrated assessment of climate change projections and snow modelling and proposes a comprehensive understanding of future changes in snow behaviours at a smaller spatial scale in different elevation zones than previously reported.

For this, we hypothesize that a warming climate and changes in rain-snow patterns would significantly alter the spatio-temporal variations of snow cover, snow water equivalent and snowmelt in the Western Himalaya. To address the hypothesis, our study derives suitable climate projections under different climate change scenarios for the 21st century and uses them for a comprehensive evaluation of changes in future snow dynamics in the small-sized Panjshir catchment in Afghanistan.

2. Materials and methods

Fig. 1 shows the methodological approach for an integrated assessment of climate change impacts on snow dynamics. The method includes three important steps: 1) Global climate model (GCM) selection and downscaling, 2) Cryospheric-hydrological modelling and 3) Future snow dynamics analysis.

A detailed description of these approaches, including a description of the study area, is provided below.

2.1. Study area

Afghanistan, located in the western Himalaya, has an arid and semi-arid climate with cold winters and hot summers. The river regime of Afghanistan depends on annual rain and snowmelt in the highlands above 2000 m a.s.l. (Qureshi, 2002). By contributing about 21% of the total river discharge in the Upper Indus basin (Lutz et al., 2014), snowmelt plays a significant role in the water supply for agriculture. Agriculture in the semi-arid climate of Afghanistan depends heavily on irrigation. The country has developed and maintained an intensive and complex multi-cropping irrigated agriculture system over the last few centuries aimed at optimizing the use of mountain waters, including snow and glacier melt, in conjunction with monsoonal rainfall (Qureshi, 2002). Snowmelt is prominent during the spring months, during which other sources of water are scarce. Similarly, both the spring and summer months correspond to the warmest seasons when the temperature is high enough to melt the remaining winter snowpack in the high-altitude regions.

The Kabul River basin is the westernmost catchment of the Indus River system. In recent decades, the temperature in the Indus basin has increased gradually, albeit with some seasonal differences (Nepal
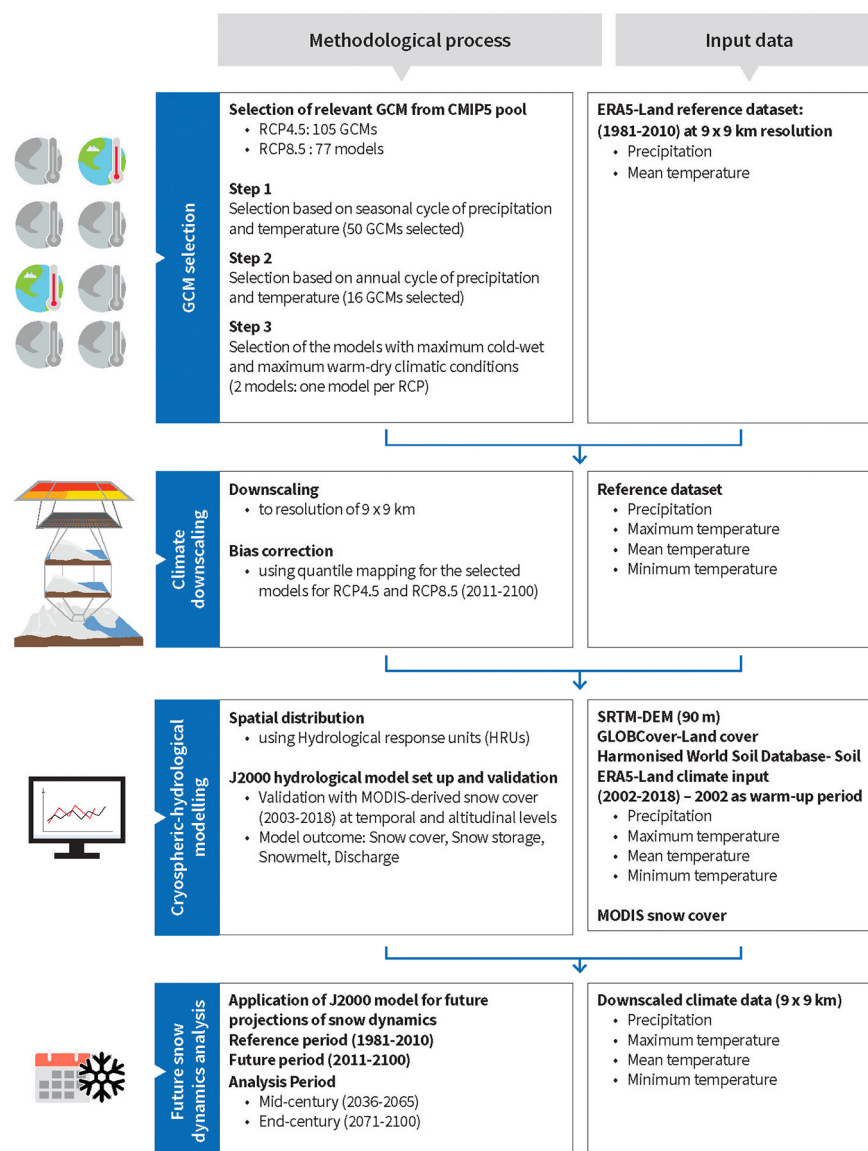

Fig. 1. Flow chart of the methodological framework for an integrated assessment of climate change impacts on snow dynamics.

and Shrestha, 2015). While Khattak et al. (2011) reported an increase in winter maximum temperature between 1976 and 2005, Rasul and Kazmi (2011) identified a significant increase in annual mean temperature from 1960 to 2007. Similarly, the average temperature in the north-western Indus basin (where the Kabul River basin is located) increased at a significantly higher rate than that of the global average during the last century (Bhutiyani et al., 2007). To what extent the temperature changes have affected snow processes in the Indus basin is yet to be quantified.

Located in northern Afghanistan, the Panjshir catchment of the Kabul River basin is the westernmost catchment of the transboundary Indus River system (Fig. 2). The main river Panjshir is 73 km long and receives streamflow contributions from nearly 20 small tributaries and streams, covering a total catchment area of 2210 km^2. The elevation in the catchment ranges between 2000 m and 5700 m a.s.l. with a mean elevation of 3500 m, forming thereby a complex system of steep mountain valleys and summits over 5500 m a.s.l. The southern Panjshir sub-basin opens onto the broad, mildly sloping, and fertile Shomali Plain, which covers important irrigated lands of about 110 km^2 in area.

The climate in the Panjshir catchment is characterised by warm-dry summers and cold-wet winters with a large spatial and temporal heterogeneity. The annual precipitation increases from the north-east to the south-west. The average annual precipitation (1981–2010) is approximately 565 mm, of which 31% occurred during winter (DJF), 42% in spring (MAM) and 13% in summer (JJA) based on ERA5-Land climate datasets (Muñoz-Sabater et al., 2021). The average annual mean air temperature of the study area is −4 °C. However, it varies from −17 °C (January) to 9 °C (August) (Fig. 2). The land cover types in the sub-basin include rangeland (86%), permanent snow and water bodies (7%), cultivated areas (3%), barren land (2%), and forest and shrub (2%).

2.2. Datasets

2.2.1. Meteorological data

Following several studies in the Himalaya region (Li et al., 2018; Lutz et al., 2016; Wijngaard et al., 2017) that used ERA based datasets, the latest meteorological data from the ERA5-Land dataset was chosen for the historical period (1981–2010) as the reference dataset. The ERA5 includes global-scale, hourly atmospheric land and oceanic climate variables that are estimated through the assimilation of several observation-based datasets into an advanced modelling data assimilation system (Hersbach et al., 2020). ERA5-Land is an improved version of the land component of the ERA5 climate reanalysis with an enhanced resolution of 9 km against the 31 km in ERA5. The temporal scale of the ERA5-Land dataset is hourly for both precipitation and average temperature (Muñoz-Sabater et al., 2021). The hourly accumulated precipitation was extracted for daily values. From the hourly temperature, daily maximum and minimum values were extracted.

2.2.2. Evaluation of input data

Due to the limited spatial coverage of meteorological observation stations in the mountainous region of the Panjshir catchment, the global ERA5-Land gridded datasets are used for spatially distributed snow simulations. The ERA5-Land dataset uses the satellite observations and meteorological observations from stations data to interpolate to a larger domain using advanced modelling and data assimilation techniques. The Panjshir catchment has only three meteorological stations (one station per 740 km^2). The stations are mostly located in river valleys and there is no coverage for high-altitude areas. Moreover, these stations cover various time periods, with one of them starting in 2009, one in 2012 and one in 2018 (Supplementary Fig. 1). For cross-evaluation of ERA5-Land, we compared the selected ERA5-Land grid with the nearest
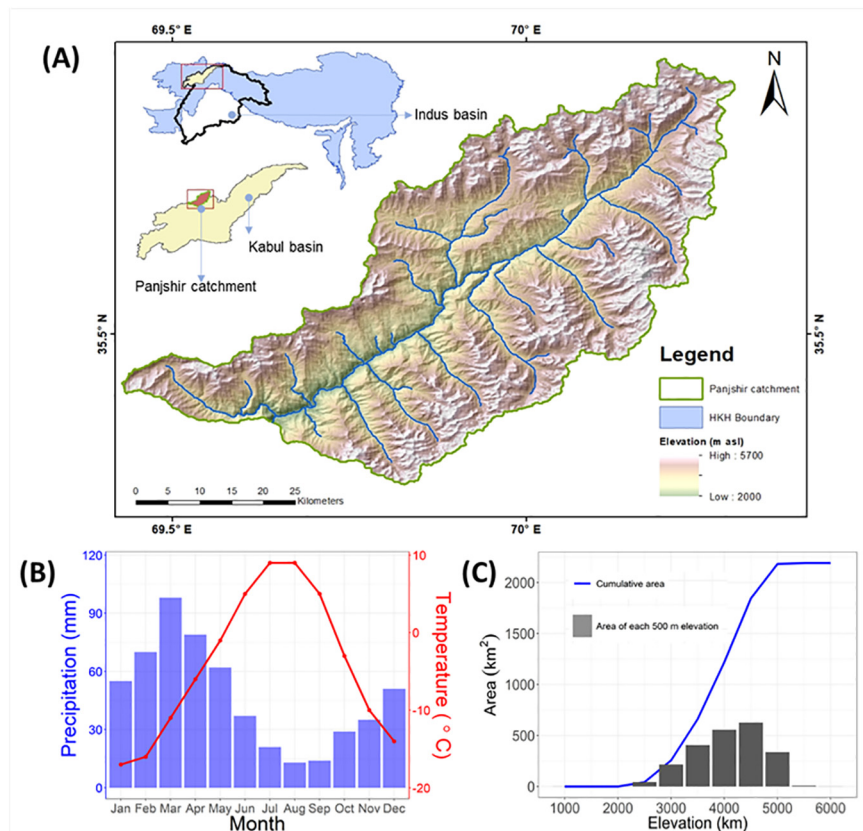

Fig. 2. Panjshir catchment of the Kabul river basin in the Western Himalaya **(A)**; Inset figure: Location of the Panjshir catchment in the Indus basin of the Hindu Kush Himalayan (HKH) region; Average monthly precipitation and temperature based on ERA5-Land (1981–2010), Data source: Muñoz-Sabater et al. (2021) **(B)**; Hypsometry of the basin **(C).**

observed station. Omarz station (station 1 in Supplementary Fig. 1), located in the southern side and low elevation zone of the basin, has the longest data record (2009–2018) and the lowest ratio of missing values. Fig. 3 shows the monthly average comparison between the ERA5-Land grid and Omarz station from 2009 to 2014. In this figure, data gaps of more than five days in a month, the monthly data of the year are excluded from the comparison.

The comparison in Fig. 3 shows that the ERA5-Land matches the monthly precipitation patterns for most of the months with a positive bias of 30%. Since stations in the mountainous region are mostly located in river valleys, the spatial variability of precipitation in the high mountains is rarely captured. Immerzeel et al. (2015) also indicated that in the upper Indus basin, the observed stations underestimate the precipitation by about 50% by considering the precipitation required to close the water balance. An advantage of ERA5-Land gridded dataset is the availability of data for a longer period and complete spatial coverage which comes particularly handy for spatially distributed modelling studies. Regarding ERA5-Land temperature, the seasonal variability matches well with observed stations, but with a negative bias in the winter season, that may be associated with elevation differences in the ERA5-Land grid and location of the station. In Fig. 3, a corrected temperature dataset is shown where the ERA5-Land mean temperature is further processed to match the elevation of the station using the global temperature lapse rate of −0.65 degree Celsius per km. Given the fair match for average monthly precipitation and temperature between the station and ERA5-Land that is comparable to previously reported ranges and biases, an additional bias correction of ERA5-Land dataset was not applied for this study.

2.2.3. Snow cover data

The snow cover data are based on the Moderate Resolution Imaging Spectroradiometer (MODIS) snow products (Hall and Riggs, 2007). They have two important advantages: (i) a long duration (18 years), which is necessary for building long-time scenarios; (ii) a robust and wide use everywhere in the world including mountain ranges, which allows comparisons with other studies. An improved daily snow cover data set developed by Muhammad and Thapa (2021) for High Mountain Asia was used to validate the model-based, simulated snow cover area. The final product is a Terra Aqua version 6 combined daily snow product – namely, M*D10A1GL06 (hereafter known as improved MODIS snow cover). This dataset improves on the original MOD10A1 (Terra) and MYD10A1 (Aqua) derived from the same sensor (Hall and Riggs, 2007) using a multi-step approach for reducing uncertainty resulting from both sensor limitation and cloud cover. Muhammad and Thapa (2021) improved the product by applying the seasonal, temporal and spatial filters to reduce snow cover overestimation, caused by large swath and lower spatial resolution, and underestimation, caused by cloud cover. The product is 99.99% cloud-free, covering the period

from 2002 to 2019 with a 500-m spatial resolution over High Mountain Asia (Muhammad and Thapa, 2021). Furthermore, the authors used MODIS MOYDGL06* eight-day product as training data for reducing the underestimation and overestimation of snow cover in daily products (Muhammad and Thapa (2020). These improved products have been used in recent studies for hydrological modelling (Bhatta et al., 2020) and snowline shifting (Khadka et al., 2020).

2.3. GCM selections and downscaling

We used simulations from several general circulation models (GCMs) from the fifth phase of the Coupled Model Intercomparison Project (CMIP5) (Taylor et al., 2012). CMIP5 promotes a standard set of model simulations to develop a collaborative framework to improve knowledge and understanding of climate change impacts. The 105 and 77 model runs, (including different models, and different realizations of the models) were available for both RCP4.5 and RCP8.5, respectively. The monthly variables were downloaded from the Royal Netherlands Meteorological Institute (KNMI) Climate Explorer (http://climexp.knmi.nl). From these model runs, the four model simulations were selected under RCP4.5 and RCP8.5 scenarios, based on their ability to reproduce the seasonal variations and means of historical climate (1981–2010) (in comparison with ERA5-Land).

- In the first step, the model selection was based on the ability of the GCMs to reproduce the historical seasonal cycle for both precipitation and temperature. Four different seasons relevant to Afghanistan were considered, namely, winter (Nov-Jan), spring (Feb-May), summer (Jun-Aug) and autumn (Sep-Oct). Percentage biases in temperature and precipitation for each model and for each season were then calculated. Eight seasonal biases (four for precipitation and four for temperature) were then averaged to rank the model runs. In this stage, about 50% of the models with the highest biases were discarded.
- In the second step, the annual biases in precipitation and temperature were calculated. The top 16 model runs with the lowest combined annual bias were chosen for the next step.
- In the third step, the changes in the magnitude of precipitation and temperature of the select models were calculated as the difference between the end-century (2071–2100) and the reference period (1981–2010) averages. This delta change encompasses the range of possible future changes in climate, from which the model runs were ranked based on the amplitude of variations under different climatic conditions. Then, the model runs with the maximum changes under warm-dry conditions and another set of model runs with the maximum changes under cold-wet conditions for RCP4.5 and 8.5 scenarios were selected (four in total). A warm-dry climate (considered a pessimistic scenario) represents extreme conditions for snow preservation as it promotes reduced snowfall and accelerated snowmelt. On the
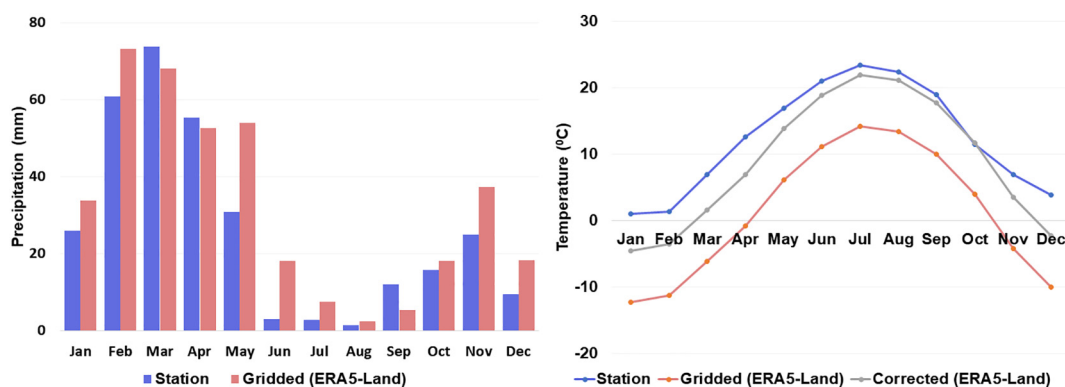

Fig. 3. Comparison between Omarz station data and ERA5-Land (Left); Average monthly precipitation (2009–2018) (Right); Average monthly mean temperature (2009–2018). Note: In the Corrected ERA5-Land data, the grid temperature was adjusted using a temperature lapse rate to the elevation of the Omarz station. (Please see Supplementary Fig. 1 for the spatial map with grids and observed stations).

contrary, a cold-wet climate (considered an optimistic scenario) represents favourable conditions for snow preservation as it promotes increased snowfall and relatively reduced snowmelt. This study considers these two spectra of future climate scenarios, using the most reasonable CMIP5 simulations, as reliable indicators of the maximum range of projected snow cover and snowmelt in the region of interest.

2.3.1. Empirical-statistical downscaling

For downscaling and bias correction, the quantile mapping method, which is a robust empirical-statistical bias correction method for mountainous regions, was used (Immerzeel et al., 2013; Themeßl et al., 2011).

The coarse resolution of current GCMs can lead to biases in climate variables, which need to be corrected through a series of downscaling processing steps. Quantile mapping adjusts the biases in climate variables from GCMs to the reference datasets at a daily resolution. In our study, this mapping was conducted, first, by applying a bilinear interpolation in space to re-grid the coarser GCM spatial resolution to the finer resolution of the reference datasets. Thereafter, the quantile mapping method was used to correct biases in the reference datasets. The correction factor was developed by applying the empirical cumulative distribution function (ECDF) between the raw GCM run datasets and the reference datasets for each month based on daily data. Correction factors, corresponding to the difference between the raw GCM values and the reference datasets, were then applied to the monthly values of the GCM datasets for the whole period (1981–2100). A similar approach to downscaling and bias correction was applied by Lutz et al. (2016) and Kaini et al. (2020).

2.4. JAMS/J2000 hydrological model

We used the standard cryospheric-hydrological J2000 model to simulate snow cover, snow storage and snowmelt processes. The J2000 model represents major cryospheric processes including snow and glacier melt processes (Nepal et al., 2014; Shen et al., 2018; Shrestha and Nepal, 2019). For snow, the model simulates snow accumulation, metamorphosis, and snowmelt processes for each spatial entity. The model has been widely used for mountain hydrological assessment at various scales ranging from micro to mesoscale catchments including snow cover simulations in the Himalayan region (Eeckman et al., 2019; Nepal et al., 2017, 2021; Shen et al., 2018), as well as in the western Himalaya (Shrestha and Nepal, 2019).

First, snow cover simulations from 2003 to 2018 were compared against MODIS snow cover data. The J2000 model was then run for the 1981–2010 period to create a reference simulation for comparison with projected periods (2011−2100). The snowfall, snow storage, and snowmelt data were used to analyse the impact of climate change on future snow dynamics. Simulated river discharge was additionally used as a multi-response outcome of the model for further discussion on the impact of snowmelt water availability on water resources and its implications for various sectoral activities.

The J2000 snow module is a component of the J2000 hydrological model, which is implemented in the JAMS Modelling System (http://jams.uni-jena.de). The J2000 snow module is able to simulate several snow-related processes such as snow accumulation, metamorphosis and snowmelt (Knauf, 1980). The snow module also considers the prognosis of the snowpack state, paying particular attention to the linkages between snow density and the process of melting and subsidence. From the described variables, sub-variables such as snow cover (i.e., the total area covered by snow), snow storage (i.e., the snow volume information) and snowmelt (i.e., the effective melting of the snowpack) are further calculated. In our study, precipitation is partitioned into rain and snow based on a threshold temperature. Depending on the cold content of the snowpack, the snowfall then accumulates on the snowpack. But the snowpack can melt when the cold content of the snowpack is higher than the threshold temperature. The model considers the energy input from air, precipitation, and soil in the form of calibration parameters to estimate the potential snowmelt. The potential snow melt is considered to be liquid water and is stored in the pore system of the snowpack until a critical snow density is reached. The melt can then either refreeze or produce snowmelt runoff. Supplementary information 1 provides a detailed description of the J2000 snow module. Krause (2001, 2002) and Nepal et al. (2017, 2020, 2021) have described the standard J2000 model in detail, including soil, groundwater and routing processes.

The resulting snowmelt is finally transferred to the soil module of the J2000 model. The maximum infiltration potential of snowmelt can be derived as another adjustable calibration parameter through which soil moisture and subsurface flow are also balanced.

2.5. Model set up, calibration, validation and uncertainty analysis

The J2000 hydrological model uses hydrological response units (HRUs) as spatial modelling entities. The HRUs were derived from the SRTM digital elevation model at the 90 m resolution, land cover data based on GlobCover (Defourny et al., 2006) and soil properties based on the Harmonized World Soil Database (FAO/IIASA/ISRIC/ISS-CAS/JRC, 2012). The DEM provides topographical properties (slope, aspect, elevation), whereas landcover properties include root depth and leaf area index for evapotranspiration. Similarly, soil data includes water holding capacity that influences infiltration, percolation, evapotranspiration and soil moisture flow. An HRU delineation workflow integrated these datasets and resulted in 7699 HRUs with an average size of 0.28 km² for the Panjshir catchment. Changes in land use and land cover conditions affect snowmelt processes (such as interception, shadow effect and infiltration). However, the projection of future land use scenarios, especially in the context of Afghanistan, is not available. Therefore, in this study, we assume the land cover properties to be fixed in time.

We used the J2000 model parameters from the previous application of the model in the Hunza catchment of the Indus basin (Shrestha and Nepal, 2019), which was calibrated and validated using both snow

Table 1
Current trends in precipitation, maximum and minimum temperature, melt days and frost days and J2000-derived snow cover (1981–2010) and improved MODIS snow cover (2003–2018).

Periods	Precipitation		Maximum temperature		Minimum temperature		Melt days		Frost days		Model snow cover[a]		MODIS snow cover	
	Trend (mm/year)	S	Trend (°C/year)	S	Trend (°C/year)	S	Days/year	S	Days/year	S	km²/year	S	km²/year	S
Spring	−0.36		0.04		0.03		0.00		0.00		−1.81		−2.24	
Summer	−0.24		0.03		0.01		0.10		−0.10		−0.53		−3.42	
Autumn	−0.13		0.06		0.06	+	0.09	*	−0.09	*	−6.02		−4.93	
Winter	0.38		0.05	*	0.04		0.00		0.00		−0.19		−9.74	*
Yearly	−1.18		0.04	*	0.03	*	0.59	*	0.59	*	−1.89		−6.16	

Note: $p < 0.001$ (***), $p < 0.01$ (**), $p < 0.05$ (*) and $p < 0.1$ (+).
S: Significance.
Melt days: Days when average of the daily maximum and mean temperature > 0 degree Celsius.
Frost days: Days when average of the daily minimum and mean temperature < 0 degree Celsius.
 [a] A discussion about the J2000 model snow cover is in Section 3.4.
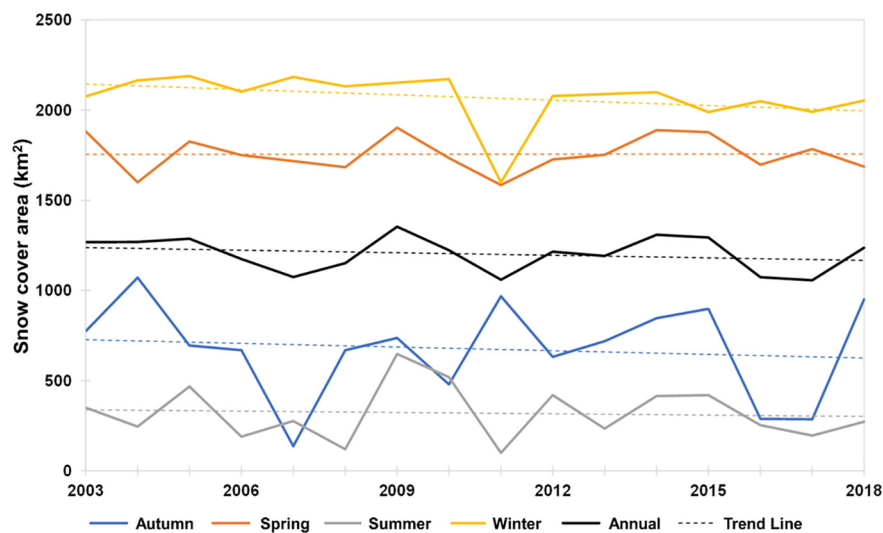
Fig. 4. Temporal patterns of seasonal and annual snow cover area based on improved MODIS data (2003–2018).

cover and discharge data. Nonetheless, a few parameters were further adjusted to match the daily MODIS snow cover. The list of calibrated parameters is provided in Supplementary Table 1. The snow-related parameters were calibrated for the period of 2003–2010, and the optimal parameters were applied for the validation of the 2011–2018 period. The model performance was evaluated using a coefficient of the determination (r^2) metric. In addition to the total snow cover over the basin, the modelled snow cover area was also evaluated across different elevation bands. Due to a lack of reliable and long-term data, the discharge simulation could not be validated independently at daily or monthly scales. While this represents a limitation, we rely on the demonstrated robustness of the J2000 model in using seasonal stream flow outputs. To obtain the complete simulation data, the validated J2000 hydrological model was forced with ERA5-Land for the reference period (1981–2010), and with high-resolution future climate projections (2011–2100) to assess the future changes in snow-related variables.

The uncertainties of the J2000 model simulations were quantified using the 10,000 Monte-Carlo simulations with random uncertainties of ±10% of the snow parameters (Supplementary Table 1). The ensemble of 10,000 simulations was used to discuss the uncertainty in the snow cover variation by applying the generalised likelihood uncertainty estimation (GLUE) as suggested by Beven and Binley (1992).

3. Results

3.1. Historical trends in climate and snow cover area

Table 1 shows trends in key meteorological variables related to snow accumulation and melting processes from 1981 to 2010. The magnitude of trends and their significance is calculated using Mann Kendall and Sen slope methods (Kendall, 1975; Mann, 1945; Sen, 1968). During this period, the maximum temperature was increasing at the rate of 0.04 °C/year and the minimum temperature at the rate of 0.029 °C/year. The increase in both minimum and maximum temperature is statistically significant at the annual scale. Similarly, precipitation is decreasing in all seasons except winter. At the annual scale, the precipitation is decreasing at 1.2 mm/year, but it is not statistically significant. Similarly, the melt days[1] are also increasing in the summer and autumn and at the annual level. Frost days[2] indicate the opposite of melt days. The

---

[1] Days when average of the daily maximum and mean temperature is greater than zero degree Celsius
[2] Days when average of the daily minimum and mean temperature is lesser than zero degree Celsius

trend in melt days indicates more than half a day of increase per year. The MODIS snow cover trend (2003–2018) indicates a decrease in snow cover area in all seasons as well as at the annual scale (Fig. 4). The decrease in winter snow cover area is about 10 km² (statistically significant) per year (Table 1). The model-derived snow cover (1981–2010) also shows a decreasing trend in all seasons and at the annual scale, but the magnitude of change is lower than the MODIS derived snow cover.

All these trends indicate that the melting process has intensified in the last 20 years. An increasing trend in temperature is also reported by many studies in the upper Indus basin (Fowler and Archer, 2006; Shahid and Rahman, 2021). On the other hand, changes in precipitation are not clear due to the lack of a significant long-term trend (Archer and Fowler, 2004; Khattak et al., 2011). As reported by Nepal and Shrestha (2015), no significant long-term precipitation trends were observed in the Indus basin, but the temporal changes are dependent on the spatial coverage, length of the data period and methods used.

3.2. GCM selection and downscaling

The GCM simulations under both RCPs were selected based on the method described in Section 2.3. Out of the 105 GCM model runs, about 50% of the model runs with the largest seasonal bias were first removed in Step 1. In Step 2, 16 model runs with the lowest annual bias in precipitation and temperature were selected for the RCP4.5 and 8.5 scenarios. The seasonal and annual bias of the selected 16 model runs is provided in Table 2. Supplementary Fig. 2 shows the monthly cycle of both selected and discarded models in the different steps, alongside the ERA5-Land reference period. While the selected GCM models reproduce the precipitation patterns of the reference datasets well, the temperature data shows a warm bias compared to the reference ERA5-Land. Such biases may result from the typical spatial scale currently available for GCMs, which is larger than that of the Panjshir catchment. As described in Section 2.3.1, these biases were corrected through quantile mapping to better match the climate seasonality of the Panjshir catchment during the reference period. In Step 3, the changes in average annual precipitation and temperature from the end of the century (2071–2100) to the reference period (1981–2010) were calculated. From the delta changes in precipitation and temperature, the models showing the maximum cold-wet and warm-dry climatic conditions towards the end of the 21st century were chosen.

Table 2 shows the seasonal (Step 1) and annual (Step 2) biases for each of the 16 selected model runs for precipitation and temperature using the ERA5-Land reference period (1981–2010). Step 3 shows differences in precipitation and temperature between the reference period

Table 2
Seasonal and annual biases of the 16 selected models, along with delta change values for precipitation and temperature discussed in Steps 1, 2 and 3 (top RCP4.5; bottom RCP8.5).

SN	Selected 16 model runs	Step 1										Step 2		Step 3	
		Seasonal precipitation bias (%)					Seasonal temperature bias (°C)					Annual precipitation bias (%)	Annual temperature bias (°C)	Delta precipitation (%)	Delta temperature (°C)
		Winter	Summer	Spring	Autumn	Pavg	Winter	Summer	Spring	Autumn	Tavg				
1	IPSL-CM5A-LR_r2i1p1	12	10	6	3	8	0.51	0.36	0.80	0.95	0.66	3%	8.9	-27.57	3.7
2	IPSL-CM5A-LR_r4i1p1	8	9	2	3	6	1.02	0.29	0.44	1.18	0.73	6%	9.0	-14.01	3.32
3	HadGEM2-ES_r1i1p1	10	9	19	0	10	0.27	0.51	2.09	1.30	1.04	2%	10.0	1.23	3.77
4	IPSL-CM5A-LR_r1i1p1	14	8	8	2	8	0.96	0.99	1.11	1.08	1.03	6%	9.1	-15.68	3.55
5	HadGEM2-ES_r3i1p1	9	9	18	1	9	0.82	0.26	2.27	1.19	1.13	4%	10.0	-2.01	3.52
6	MRI-CGCM3_r1i1p1	8	7	6	9	7	1.54	1.61	1.01	1.08	1.31	2%	10.6	7.04	2.57
7	HadGEM2-ES_r4i1p1	9	10	19	1	10	1.21	0.15	2.24	0.88	1.12	4%	10.2	9.12	3.09
8	IPSL-CM5A-LR_r3i1p1	13	9	7	3	8	0.60	0.61	1.12	1.10	0.86	8%	9.1	-12.24	3.39
9	HadGEM2-CC_r1i1p1	9	10	17	2	9	0.94	0.71	2.62	0.97	1.31	8%	9.6	10.83	3.25
10	CNRM-CM5_r1i1p1	7	4	5	6	5	2.69	2.04	0.40	0.25	1.34	7%	9.7	1.91	2.88
11	Inmcm4_r1i1p1	1	6	0	7	3	0.24	0.05	3.24	2.95	1.62	24%	6.5	-14.59	1.64
12	HadGEM2-AO_r1i1p1	11	8	18	1	10	0.67	0.45	2.19	1.07	1.09	10%	10.6	-0.06	3.82
13	CMCC-CMS_r1i1p1	5	12	6	0	6	0.73	1.78	2.15	1.10	1.44	12%	10.2	-14.11	3.32
14	MIROC-ESM-CHEM_r1i1p1	2	3	7	2	4	0.15	0.47	1.00	1.32	0.74	5%	12.2	-4.54	3.96
15	GFDL-CM3_r1i1p1	1	9	4	4	4	1.04	1.02	0.29	0.27	0.65	19%	9.0	-22.28	4.65
16	ACCESS1-0_r1i1p1	10	8	15	2	9	0.14	0.52	2.51	1.85	1.26	18%	9.7	2.87	3.5

SN	Selected 16 model runs	Step 1										Step 2		Step 3	
		Seasonal precipitation bias (%)					Seasonal temperature bias (°C)					Annual precipitation bias (%)	Annual temperature bias (°C)	Delta precipitation (%)	Delta temperature (°C)
		Winter	Summer	Spring	Autumn	Pavg	Winter	Summer	Spring	Autumn	Tavg				
1	IPSL-CM5A-LR_r2i1p1	12	10	5	3	7	0.65	0.26	0.70	1.09	0.67	0%	9.0	-36.97	6.8
2	IPSL-CM5A-LR_r4i1p1	8	9	3	4	6	1.06	0.35	0.49	1.20	0.77	5%	8.9	-38.02	7.03
3	MRI-CGCM3_r1i1p1	8	7	6	8	7	1.50	1.55	0.95	1.00	1.25	1%	10.7	13.7	5.01
4	IPSL-CM5A-LR_r3i1p1	12	9	7	4	8	0.61	0.70	1.04	0.95	0.82	8%	9.1	-27.69	6.71
5	IPSL-CM5A-LR_r1i1p1	15	9	7	1	8	0.82	0.99	1.11	0.95	0.97	8%	9.1	-25.89	6.57
6	HadGEM2-ES_r3i1p1	9	10	17	1	9	0.74	0.18	2.15	1.24	1.08	5%	10.0	6.07	6.25
7	CNRM-CM5_r1i1p1	7	3	4	6	5	2.64	1.85	0.55	0.23	1.32	6%	9.9	11.52	4.79
8	Inmcm4_r1i1p1	0	7	0	7	3	0.34	0.05	3.11	2.71	1.56	22%	6.4	-21.14	3.95
9	MIROC-ESM-CHEM_r1i1p1	0	4	7	2	3	0.24	0.52	1.12	1.40	0.82	3%	12.2	-13.02	6.86
10	HadGEM2-AO_r1i1p1	11	8	18	1	9	0.45	0.53	2.07	1.09	1.03	10%	10.6	4.83	5.67
11	CMCC-CMS_r1i1p1	7	12	6	1	7	0.50	1.58	2.15	1.07	1.32	13%	10.2	-17.42	6.16
12	GFDL-CM3_r1i1p1	1	9	5	3	4	0.92	0.97	0.17	0.22	0.57	18%	9.0	-17.45	7.37
13	ACCESS1-0_r1i1p1	9	8	16	2	9	0.08	0.59	2.54	1.88	1.27	18%	9.8	3.21	5.64
14	MIROC-ESM_r1i1p1	2	2	6	3	3	0.00	0.29	1.09	1.37	0.69	9%	12.2	-19.07	6.88
15	MIROC5_r2i1p1	5	12	10	2	7	1.41	0.61	1.34	0.55	0.98	19%	12.7	2.8	5.34
16	MIROC5_r1i1p1	6	13	10	3	8	1.14	0.55	1.41	0.81	0.98	19%	12.8	2.07	5.45

and the 2071–2100 period. In Step 3, based on delta changes in precipitation and temperature, the models representing the maximum warm-dry and cold-wet conditions (highlighted in green) were selected for high-resolution downscaling.

Based on the method described in Section 2.3, the selected models were downscaled and bias-corrected to high-resolution data of 9 × 9 km resolution. Table 3 shows the changes in temperature and precipitation values after downscaling, highlighting the selected model runs and their respective projections for the Panjshir catchment by the mid- and end-century compared to the reference period. These high-resolution data were used to analyse climate change scenarios and to force the J2000 hydrological model to simulate future snow behaviour (see Supplementary Fig. 3, which shows the raw GCM data vs. bias-corrected data on a monthly scale).

3.3. Future climate scenarios

After downscaling the GCM simulation, high-resolution temperature and precipitation data for 51 grid points of the Panjshir catchment were obtained. Fig. 5 and Table 3 show the future changes in precipitation and mean temperature for cold-wet and warm-dry climatic conditions for RCP4.5 and RCP8.5. The figure shows that there is clear agreement among models for increasing temperature scenarios. All models project an increase in annual mean temperature towards the end of the century, with larger changes in RCP8.5 compared to RCP4.5. However, regarding precipitation, the models exhibit a much larger spread with both increasing and decreasing patterns (depending on the climatic conditions). Compared to temperature, precipitation projections are not uniform, as the model selection also prioritises models with a decrease in

precipitation under a drier climate. In general, the models indicate that the Panjshir catchment is likely to get warmer in the future, with a large degree of variability in terms of precipitation characteristics. Table 3 shows the change in future temperature and precipitation for both climatic conditions under both the RCPs. According to the projection, the mean temperature could increase by 2.5 °C (cold-wet, RCP4.5) to 7.8 °C (warm-dry, RCP8.5) by the end of the 21st century. In the case of precipitation, an increase by 28% and a decrease by 40% can be expected for cold-wet and warm-dry conditions, respectively, under RCP8.5.

3.4. Modelling snow cover

The application of the J2000 model provided detailed spatial and temporal information on snow cover. For a given HRU, when the snow cover is higher than 5 mm, the HRU is treated as snow covered area, and as snow-free area otherwise. Fig. 6 shows the daily snow cover

Table 3
The selected model runs and their respective projections in terms of temperature and precipitation changes for the Panjshir catchment by mid- and end-century compared to the reference period.

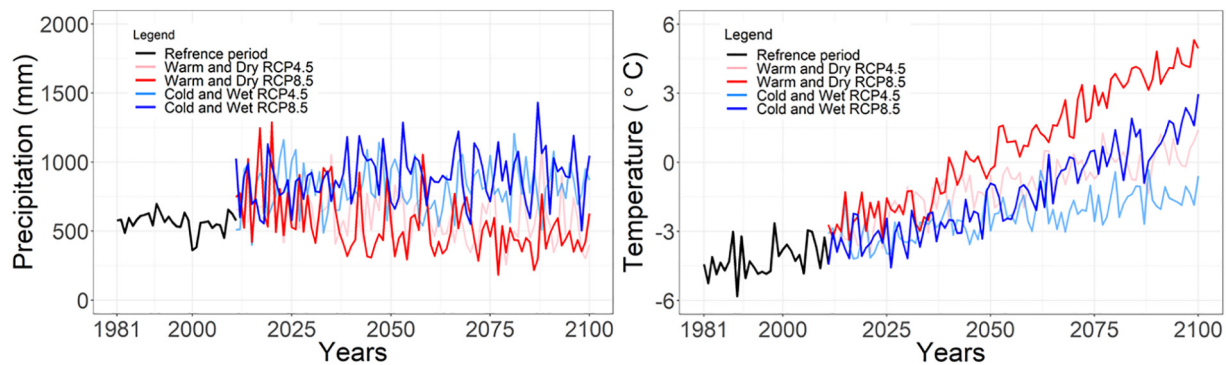| RCPs	Model characteristics	Model names	Mid-century		End-century	
			P (%)	T (°C)	P (%)	T (°C)
RCP4.5	Cold and wet	MRI-CGCM3_r1i1p1	4	1.9	13	2.5
	Warm and dry	IPSL-CM5A-LR_r2i1p1	−17	3.1	−26	4.3
RCP8.5	Cold and wet	MRI-CGCM3_r1i1p1	23	2.2	28	4.9
	Warm and dry	IPSL-CM5A-LR_r4i1p1	−34	4.4	−40	7.8

Fig. 5. Future changes in precipitation and temperature in the Panjshir catchment. The black line represents ERA5-Land reference datasets (1981–2010).

plots derived from MODIS and the J2000 hydrological model for the calibration (2003−2010) and validation (2011–2018) periods. The model matches the MODIS snow cover for both the calibration and validation periods as shown in Fig. 6. Fig. 6A shows daily snow cover data from both MODIS and the J2000 model. The coefficients of determination (r^2) are 0.93 and 0.95 for the calibration and validation periods, respectively. The average monthly snow cover also shows a good match during the snowmelt period, while the modelled accumulation is slightly underestimated during the Aug-Oct period and overestimated during the winter months (Nov-Jan) (Fig. 6C). Overall, the average annual percentage bias of model-derived snow cover is 10% higher than MODIS. These discrepancies can be attributed to the different processing methods used by MODIS compared to the J2000 model and different spatial resolutions.

Furthermore, we compared the modelled and MODIS snow cover across 500-m elevation bands in the Panjshir catchment. In Supplementary Fig. 4 the comparison between the fraction of snow-covered area from J2000 (model) and improved MODIS snow cover (MODIS) for each elevation band is shown. Overall, the model outcome compares well with that of MODIS datasets between 2500 and 5000 m, where the r^2 ranges between 0.70 and 0.90. However, below 2500 and above 5000 m, the r^2 range is 0.63 and 0.18, respectively. Overall, the model reproduces the snow cover variation across all elevation bands except for higher than 5000 m. However, the area above 5000 m is very low (11.5 km^2) which may be the reason of higher variation in that elevation band.

Fig. 6D shows the average daily variation in snow cover from 2003 to 2018. The grey band shows the maximum and minimum snow cover area of each day between the year (from 2003 to 2018). Across the years, the variation is smaller during the melting period (spring and summer) than during the autumn and winter seasons, as shown by peaks around days 240 to 300. Such variation can be attributed to sudden winter snowfall events. The largest variability in snow cover throughout the year is during the winter season, from days 280 to 340, whereas the lowest variability is during the peak of winter (Jan-Feb) when the basin is fully snow-covered during most years.

3.5. Snow storage and snowmelt

Snow storage (or snow water equivalent in mm) and snowmelt are provided in Fig. 7. Snowmelt is the highest in June while snow storage reaches its peak in March–May. The lowest snow storage is from August to September, which matches the lowest snow cover period at the end of summer. While snow storage increases from October to April due to increased snowfall, it decreases from May to August mainly because of increasing temperatures, which cause faster melting.

Fig. 7 (top) shows the average monthly solar radiation and the maximum temperature. At the basin scale, the maximum temperature reaches above 0 degree Celsius values from May, when solar radiation becomes significant, until it reaches its maximum during July and

August when solar radiation is at its highest. Fig. 7 (bottom) shows the average monthly snow storage and snowmelt. The snow storage is the highest in April, starts to decrease in May, and reaches its minimum in September. Similarly, snow starts to melt in March until June, when it reaches its maximum (about 6 mm/day). As illustrated in Fig. 7, the melting season (i.e., March–July) coincides well with the period of maximum solar radiation and higher temperature.

3.6. Uncertainty analysis

Fig. 8 shows the 10,000 simulations of uncertainty analysis for snow parameters using the Generalised Likelihood Uncertainty Estimation (GLUE) method (see Supplementary Table 1 for the parameters values). In order to constrain and optimise the Monte Carlo simulations used in this method, parameter values were randomised within a ± 10% range. For the sake of clarity, however, only 25% of simulations of the most recent years are plotted (Fig. 8) (see Supplementary Fig. 5, which shows simulations for the entire period). In most cases, the MODIS-derived snow cover, for both accumulation and melting seasons, lies within the uncertainty range (mostly around the lower boundary), suggesting that the snow parameters considered here are mainly conducive to snow cover development. Since the snow cover melts when the temperature rises, the lower boundary is very close to the observed MODIS datasets. However, in some years, for e.g., 2015 and 2016, the MODIS maximum snow cover is outside the uncertainty range (see also Supplementary Fig. 5). The parameter uncertainty is also at its highest during the melt phases whereas snow accumulation and maximum extent are much less affected by parameter uncertainty. Nevertheless, the coefficient of determination (r^2) between MODIS data and the median value of ensemble runs for the entire period (2003–2018) is 0.91, suggesting a low degree of uncertainty in the results. These considerations from our GLUE-based uncertainty analysis confirm the robustness of the J2000 model in estimating snow cover in the Panjshir catchment.

3.7. Changes in snowfall

Table 4 summarizes the changes in snowfall in the mid-century and end-century compared to the reference period (1981–2010). The largest reduction in snowfall is projected to occur during the summer and autumn seasons. In the cold-wet scenario, the snowfall is likely to increase slightly in winter and spring though likely to decrease to a large extent in summer and autumn (Table 4). In the warm-dry scenarios, the snowfall is likely to decrease in all seasons. For example, in the summer season, snowfall is likely to decrease by about 55–75% in cold-wet and 70–94% in warm-dry scenario by the end of the century. In all simulations, the snowfall amount will decrease in the Panjshir catchment in the summer and autumn seasons, irrespective of the model type and related climate.
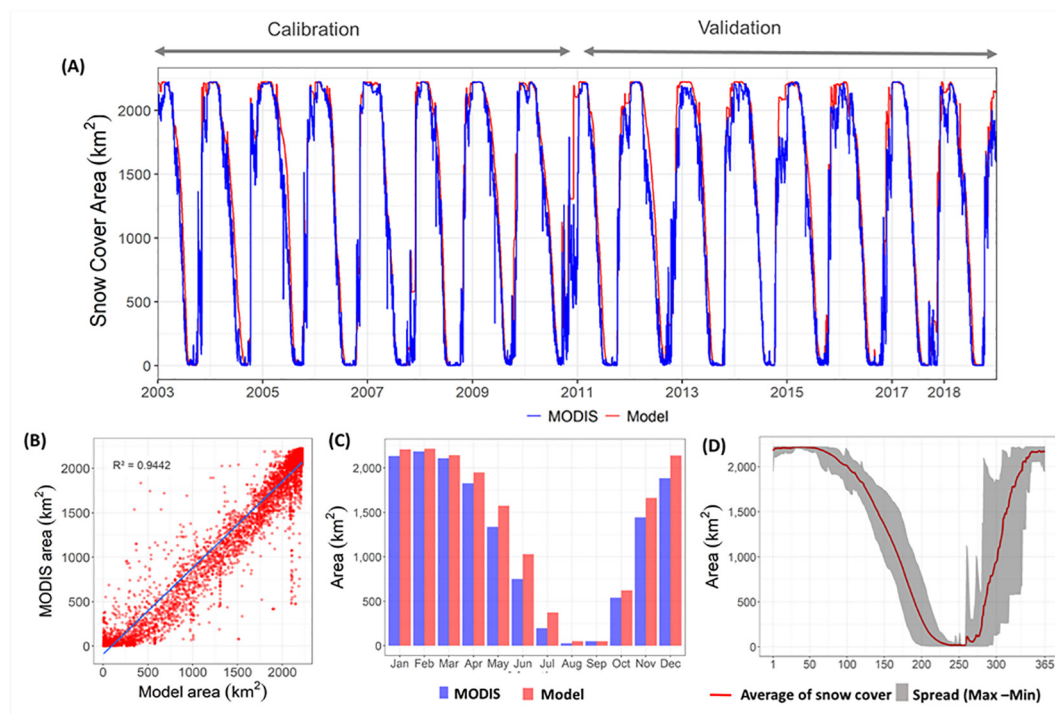
Fig. 6. Daily snow cover in the Panjshir catchment derived from the J2000 model and improved MODIS dataset (Muhammad and Thapa, 2021). A) Daily snow cover area from improved MODIS vs. J2000 Model; B) Scatter plot of improved MODIS vs. J2000 model; C) Long-term average monthly snow cover; D) Daily variation of snow cover from 2003 to 2018 based on the J2000 model.

3.8. Decadal snow cover trend

Fig. 9 shows the monthly-scale decadal snow cover scenario from the 2010s to the 2090s. When the whole range of possible climatic conditions is taken into consideration, the snow cover in the Panjshir
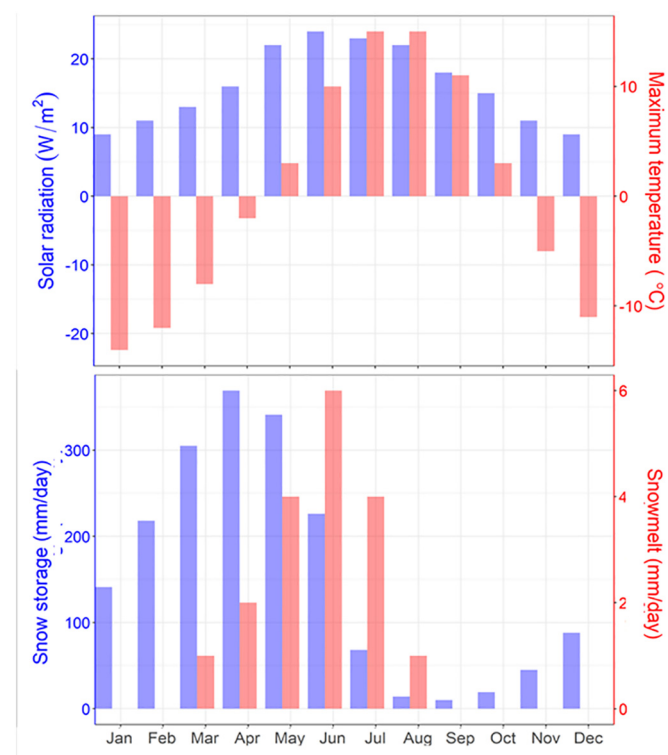
Fig. 7. Average monthly solar radiation, maximum temperature, snow storage and snowmelt during 2003–2018.

catchment is projected to decrease in almost all months. This is especially evident during the melting (Apr-Jun) and accumulation seasons (Sep-Feb). It is also observed that the most adverse climatic conditions for snow cover in the future are in the warm-dry scenario. Similarly, the changes in snow cover are more pronounced under RCP8.5 than under RCP4.5 scenario. For example, in a warm-dry model under RCP8.5, the snow-covered area is predicted to become snow free from June to October when compared to approximately 750–1000 km^2 during the reference period.

3.9. Trends in seasonal snow cover

Fig. 10 and Table 5 show the seasonal snow cover trends for the four seasons: winter (Dec-Feb), spring (Mar-May), summer (Jun-Aug) and autumn (Sep-Nov). They show that seasonal snow cover is projected to decrease in all four seasons throughout the 21st century. Under all climatic conditions considered, the maximum snow cover loss amounts to about 25% on average during spring and autumn. Even with the most optimistic climatic conditions (i.e., cold-wet climate), the snow cover loss amounts to approximately 10% and 15% in the spring and autumn seasons, respectively. At the annual scale, the snow cover area is projected to decrease by 1.6 to 3.2 km^2/year in the cold-wet models compared to 3.9 to 6.2 km^2/year in the warm-dry models (see Supplementary Fig. 6). At such rates, the snow cover in the Panjshir catchment is likely to decrease from 10% in the cold-wet models in RCP4.5 to 36% in the warm-dry model in RCP8.5, with an average decrease of 22%. Conditions would become particularly harsh in case a warm-dry condition were to prevail, as the average annual snow cover would decrease to less than half of the reference period (1981–2010) by the end of the century.

3.10. Altitudinal changes in snow cover

Fig. 11 shows the future snow cover area projections in different elevation zones for the mid-century (2036–2065) and end-century (2071–2100) periods. The figure suggests a consistent decrease in snow cover across all elevation bands (2000–5500 m a.s.l.) compared to the
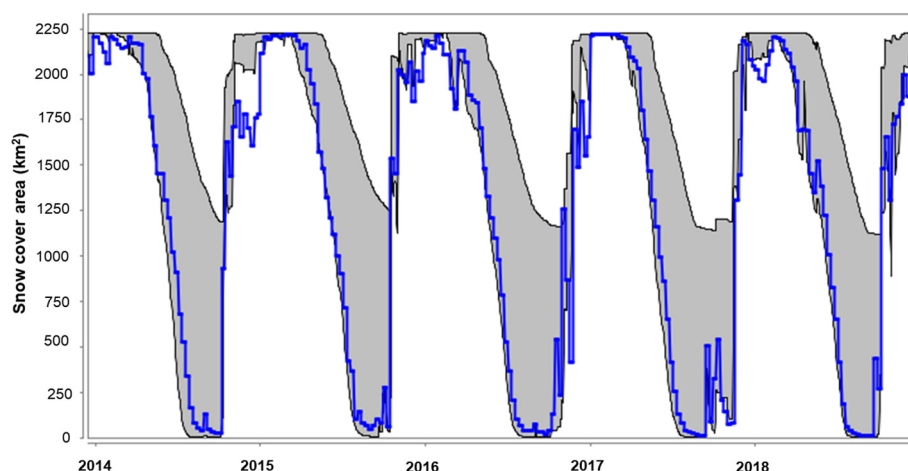
Fig. 8. Generalised Likelihood Uncertainty Estimation (GLUE) from 10,000 simulations. The grey band shows the ensemble simulation range; the blue line indicates the MODIS snow cover. (For interpretation of the references to colour in this figure legend, the reader is referred to the web version of this article.)

reference period (1981–2010). The snow cover is projected to decrease in the high elevation zones (above 4500 m a.s.l.) by more than 60% between the months of June and November (with no snow cover in August and September) in the warm-dry condition of RCP8.5 scenario by the end-century. In the low elevation zones below 3000 m a.s.l, over 50% of the snow cover area will decrease from December to February in the warm-dry condition of RCP8.5 scenario. Even in the cold-wet condition of the RCP4.5 scenario, there will be a decrease in snow cover area in the high elevation zones by roughly 10% between the months of June and November and by roughly 20% between the months of December and February by the end-century. Furthermore, the reduction in snow cover in the winter season will be more noticeable in the lower elevation areas than in the high elevation areas and this pattern is projected to strengthen towards the end-century. In high elevation areas, snowmelt will start earlier in the year than before. For example, at 5000–5500 m a.s.l., the start of the snow cover decline will shift from June to April and will continue till

September by the end-century as projected in the warm-dry condition of the RCP8.5 scenario; the snow cover will correspondingly decrease to ~75% of that of the reference period. Similarly, in low elevation zones, the snowmelt is expected to advance by a month in most scenarios. In the extreme case of warm-dry conditions, all elevation bands will be nearly devoid of snow throughout the July–September period under the RCP8.5 scenario. Although all our simulations point to unfavourable conditions for the development of snow, our results confirm the idea that the largest percentage of snow cover reduction will occur towards the end-century period under RCP8.5 and in case of warm-dry projections.

3.11. Snow storage and snowmelt

Fig. 12 shows the snow storage and snowmelt for the mid-century and end-century periods under cold-wet and warm-dry conditions.

Table 4
Changes in snowfall (mm) in the mid-century (2036–2065) and end-century (2071–2100) compared to the reference period (1981–2010) for selected climate scenarios.

| Periods	Cold and Wet RCP4.5	Cold and Wet RCP8.5	Warm and Dry RCP4.5	Warm and Dry RCP8.5
Winter (DJF)				
Reference	247	247	247	247
Mid-century	277	294	192	204
End-century	276	301	205	205
Spring (MAM)				
Reference	284	284	284	284
Mid-century	259	326	234	174
End-century	309	297	193	128
Summer (JJA)				
Reference	33	33	33	33
Mid-century	20	20	25	11
End-century	15	8	10	2
Autumn (SON)				
Reference	92	92	92	92
Mid-century	87	96	53	37
End-century	77	81	50	18
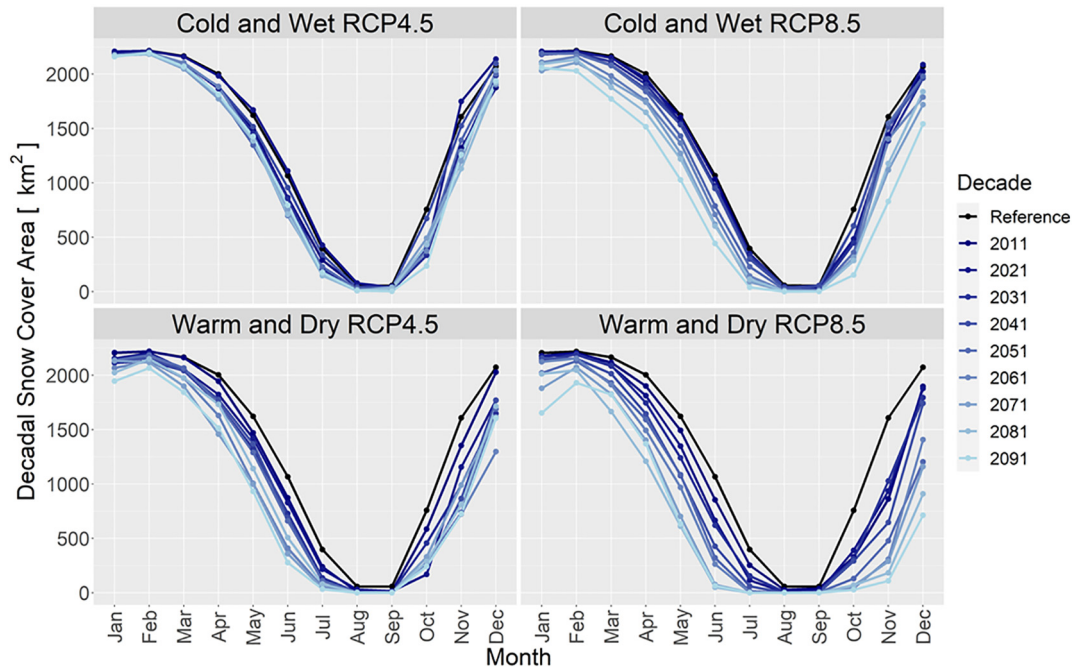
Fig. 9. Decadal snow cover changes in the Panjshir catchment for cold-wet and warm-dry climatic conditions for selected climate scenarios compared to the reference period (1981–2010).

The cold-wet models indicate that snow storage is likely to increase under these conditions around the mid-century and slightly decrease at the end-century periods, except during the summer season. In summer, the snow storage is likely to decrease during both the mid- and end-century periods. In the warm-dry models, however, there is a consistent decrease in snow storage in the mid-and end-century periods under both RCP4.5 and RCP8.5 scenarios, with an even stronger propension for snow storage reduction under RCP8.5. The largest decrease in snow storage is projected for summer when the snow storage is nearly zero by the end-century under the RCP8.5 scenario. Compared to the reference period, all seasons show almost one-third reduction in

snow storage under RCP4.5 and approximately 50% reduction in snow storage under RCP8.5.

With regard to snowmelt, as with snow storage, the cold-wet models display a consistent increase in snowmelt in all seasons towards the end-century except during summer. The maximum increase is observed in the winter season when snowmelt increases to about 40 mm on average in the end-century and RCP8.5 scenarios compared to 4 mm during the reference period. In the warm-dry models, winter and spring display a consistent increase in snowmelt with a bigger increase in winter whereas summer and autumn seasons display the opposite trend, with a consistent decrease in snowmelt with a bigger
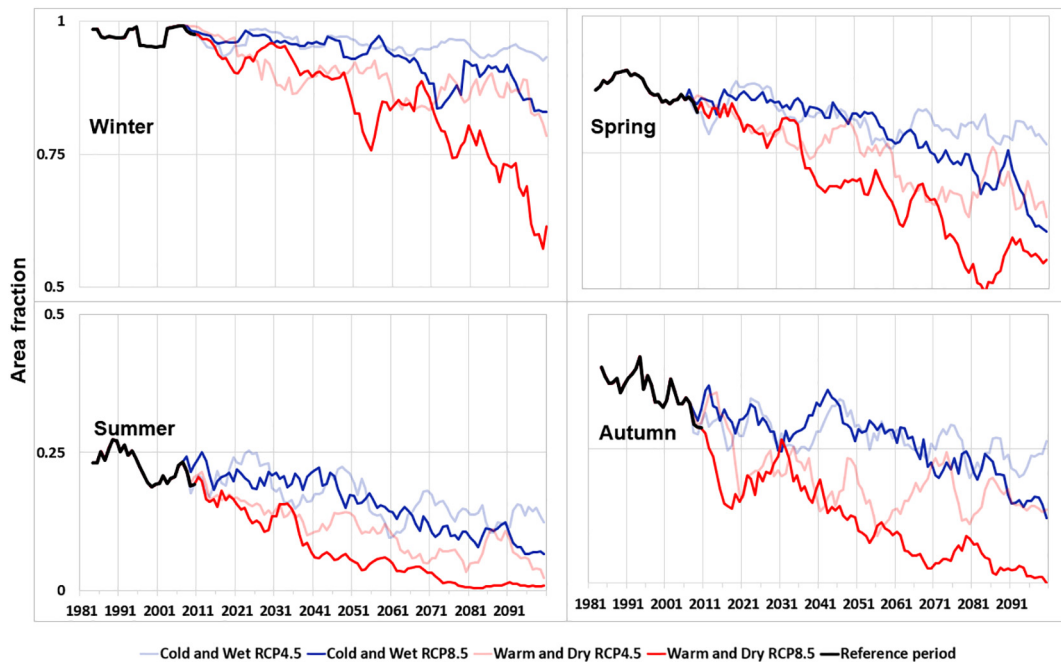

Fig. 10. Seven-year moving averages of seasonal snow cover for climate projections under RCP4.5 and 8.5 scenarios. The black line stands for snow cover estimation based on ERA5-Land reference period (1981–2010).

Table 5
Changes in snow cover in different seasons for RCP4.5 and RCP8.5.

Seasons	Cold and wet RCP4.5	Cold and wet RCP8.5	Warm and dry RCP4.5	Warm and dry RCP8.5	Average
Winter	−4%	−12%	−16%	−33%	−16%
Spring	−10%	−23%	−25%	−40%	−25%
Summer	−12%	−18%	−21%	−29%	−20%
Autumn	−15%	−22%	−27%	−42%	−26%
Annual	−10%	−18%	−22%	−36%	−22%

decrease in summer. Overall, irrespective of the model characteristics, winter and spring seasons are likely to witness an average increase in snowmelt by 6.7 and 1.3 times respectively in the future because of increased temperature. The summer season, in contrast, is likely to witness a decrease in snowmelt by 0.5 times on average due to decreased snow storage.

4. Discussion

Under the current climate change projections for the Panjshir catchment, temperatures are expected to become significantly higher whatever the scenario, thereby inducing accelerated melting and a decreasing snow cover. Because of the higher temperature increase projected under RCP8.5 than under RCP4.5, all RCP8.5 simulations show a larger decrease in snow cover during all seasons compared to that under the RCP4.5 scenario.

Additionally, when considering the evolution of snow cover across the full range of elevation bands, our study suggests that both the lower and higher elevation zones will be subjected to a larger decrease in snow cover area than the mid-elevation zones. In the lower elevation zones, the precipitation phase will be more susceptible to a shift from snow to rain because of higher air temperatures. The aggravated decrease in snow cover in the elevation bands below 3000 m a.s.l. could be attributed to the same reason. In the lower elevation areas, the snowmelt patterns are likely to remain unchanged. In the higher elevation areas (i.e., above 5000 m a.s.l.), on the other hand, the snowmelt season is expected to begin at least 1 or 2 months earlier than during the reference period while the magnitude of snowmelt will be larger under RCP8.5 than the increase projected under RCP4.5. Furthermore, the expected overall decrease in snowfall, especially during the summer and autumn seasons, can be attributed to changes in precipitation form, which will switch from snow to rain more often.

Another finding of this study, determined by the selection of GCMs and their associated climates, is that the cold-wet models project more snowfall than the warm-dry models during all seasons except summer. In the warm-dry scenario, because of the higher increase in
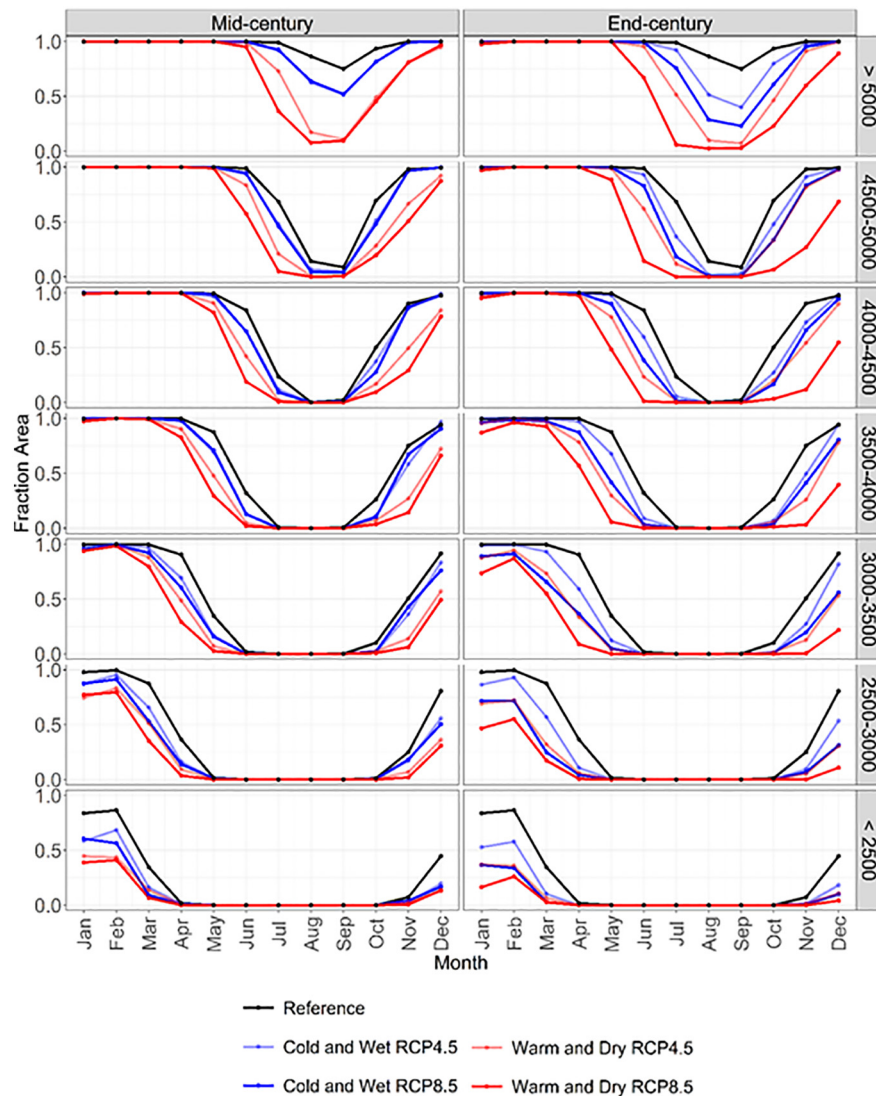

Fig. 11. Changes in future snow cover in different elevation zones of the Panjshir catchment for the mid-century and end-century periods for selected climate scenarios compared to the reference period (1981–2010).
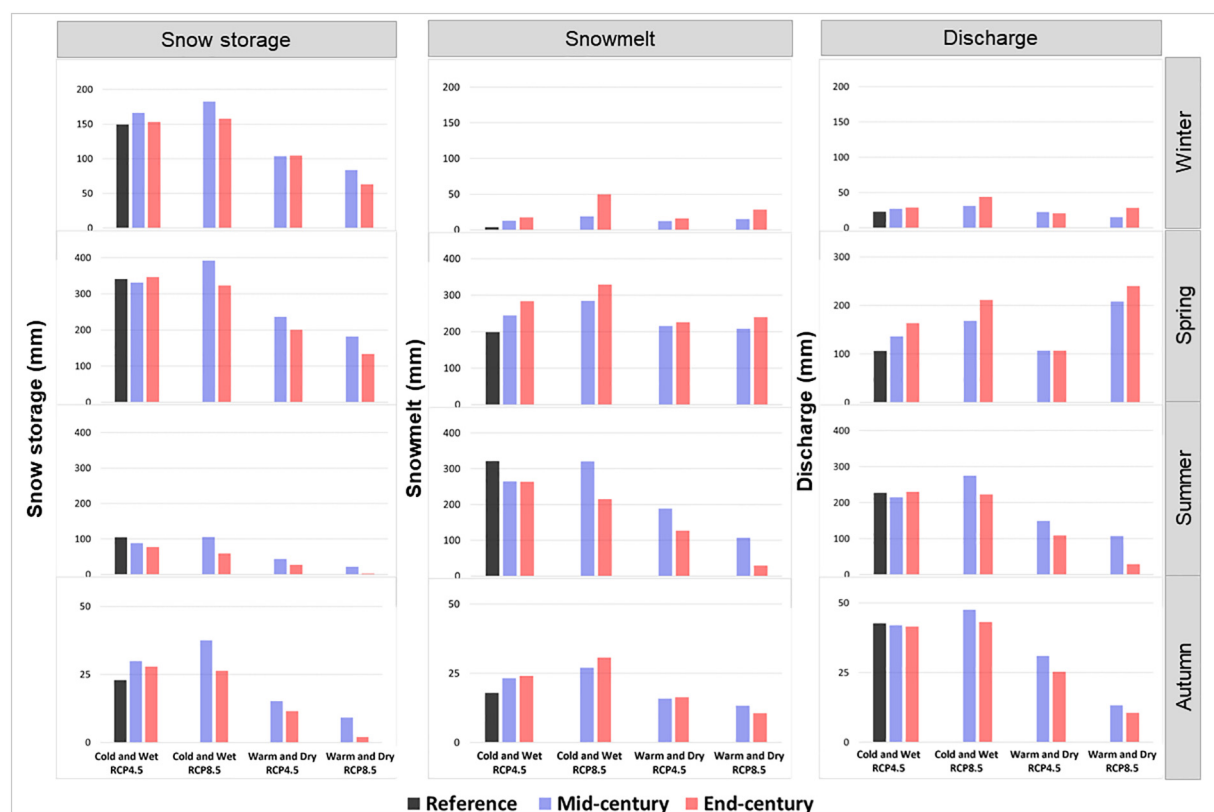
13

Fig. 12. Future changes in snow storage (left), snowmelt (middle) and runoff (right) during the mid-century and end-century compared to the reference period (1981–2010).

temperature, a larger proportion of precipitation will fall as rain. The magnitude of this increase in temperature is higher in the RCP8.5 scenarios than in RCP4.5 scenarios, which will ultimately lead to a more severe snow storage reduction for all the climates considered (Table 4).

Another effect of increased temperature is a significant increase in snowmelt intensity during the winter and spring seasons by the end of the 21st century, when all climatic conditions are considered. In the reference period, snow is already only sparsely available for melt during the summer season. This reduction of snow in the summer is projected to further exacerbate in the future as there will not be much snow left to melt in the summer months because of the melting of the snowpack already in the spring season (Figs. 9 and 12). In the autumn season, on the other hand, depending on the type of prevailing climate, snowmelt will vary in intensity significantly. In cold-wet conditions, as more snow will fall in the catchment, the snowmelt intensity too will increase as a result of associated increasing temperatures compared to the reference period. In the case of warm-dry conditions, however, snowmelt intensity will decrease owing to reduced snowfall. Future melt runoff is also expected to peak one month earlier in May rather than June, as is the case in the reference period) by the end of the century except in the cold-wet scenario of RCP4.5 (see Supplementary Fig. 7). The river discharge pattern will follow the melt runoff patterns, the latter being characterised by either an increase in intensity during winter and spring seasons or a decrease during summer. Several studies have documented similar trends in winter and summer patterns in various mountainous regions of the world, which have been attributed to a shift from snow to rain in precipitation under warmer conditions (Hock et al., 2019).

The results of our analysis finally suggest that changed climatic conditions during winter and spring seasons would enhance snowmelt and runoff, which could alter the agricultural and livelihood practices of the people in the Panjshir catchment owing to the combined effects of increased water availability, soil moisture and groundwater recharge. On the other hand, the strong reduction in snowmelt-driven runoff projected for the summer could reduce water availability. Since spring

temperatures will also increase in the future, one adaptation strategy, among others, to cope with the climatic changes described above, would be to plant summer crops early by making use of the early melt runoff available. However, such a shift in agricultural practices would certainly require the implementation of adequate consultation mechanisms with local communities and authorities, together with proper crop monitoring and assessment in the Panjshir catchment.

4.1. Uncertainty and limitations

Projecting future climates is a complex task, especially in sparsely documented and observed regions. This is not only because of the multitude of factors creating uncertainty in GCMs and climate projections but also because of the limited understanding of current socio-economic pathways and their constant evolution. One way of dealing with such uncertainty about the future is to develop a range of plausible scenarios based on the present understanding of climatic conditions. Based on this idea, two extreme future scenarios relevant to snowmelt, i.e., cold-wet and warm-dry climates, were selected for this study. While other climate conditions might prevail in the future (e.g., warm-wet), we limited our study to the warm-dry and cold-wet endmember climatic standpoints from a spectrum of possible scenarios affecting snow processes. Discussions related to runoff should also be interpreted considering the limitations in our study, as the discharge output from the J2000 model could not be validated independently with the measured discharge data. The results of our uncertainty analysis related to the model parameters suggest that the improved MODIS snow cover datasets remain within the parameter uncertainty range, and thus can be considered as low (Fig. 8). However, it should be noted that there are inherent factors contributing to uncertainties in the snow-cover products, e.g., resulting from the large spatial resolution of satellite observation, cloudiness and saturation of signal (Muhammad and Thapa, 2020).

As the assessment of climate change impact on snow cover (and other environmental variables) are subject to uncertainties with the

model projections, our study uses two extreme changes, i.e., warm-dry and cold-wet, and assumes that the extremes bracket the uncertainties across the models. Considering the long-term end-century scenarios and the multiple possibilities of divergences from the initial hypothesis, a detailed uncertainty analysis is unwarranted, and the result of this study should be taken as a possible trend.

5. Conclusions

Given the crucial significance of snow as an integral component of the hydrological cycle in mountainous regions of the world, how snow processes evolve under climate change is a paramount question in the western Himalayan region. The integrated assessment of snow projection scenarios for the Panjshir catchment in Afghanistan conducted in this study enabled us to explore this question and to investigate the effect of climate change on snow dynamics throughout the 21st century using the J2000 cryospheric-hydrological model. We focused on investigating the changes in snowfall, snow cover, snow storage and snowmelt based on two possible endmember future scenarios, representing, namely, cold-wet and warm-dry climates. These two climatic scenarios were specifically selected as they reflect the opposite spectrum of climate impact on snow processes: cold-wet conditions will likely favour enhanced snowfall and reduced snowmelt in the basin while warm-dry conditions will lead to significantly reduced snowfall and enhanced melt.

A consistent decrease in decadal snow cover area in particular shows that the basin's snow storage capacity will be reduced in the future compared to the reference period. Likewise, the seasonal snow cover analysis suggests that all seasons will lose snow in various degrees, especially during spring and autumn in a warm-dry scenario. Though decreasing snow cover patterns are evident in all elevation bands, a noteworthy feature from our study is that snow cover melting will be initiated at least one month earlier than that during the reference period, particularly above 5000 m a.s.l., while the largest snow cover reduction will occur in lower elevation areas (Fig. 11). These results support our hypothesis that the warming climate and changes in rain-snow patterns could impact snow evolution towards the end of the century and impact melt runoff patterns.

The projected future changes in snow dynamics for the Panjshir catchment lead to new challenges in adapting to the impacts of climate change for water-dependent sectors. There are implications for water provisioning, mountain ecosystems and agriculture at the local and regional scales. Hock et al. (2019) and Nie et al. (2021) also highlighted that changes in snow and glacier related melt runoff can have local impacts on water resources, agriculture, biodiversity and overall ecosystems in mountain regions. Likewise, our projection of an increase in winter melt runoff and a decrease in summer melt runoff suggests a need for the development of adaptation mechanisms in existing agricultural practices based on the future evolution of snowmelt runoff timing that considers the need to use excess melt runoff in the spring to overcome the negative effects of reduced melt runoff in the summer. Given the robustness of the method adopted throughout our study and its use of globally and freely available datasets, this approach can be transferred to other snow-dominated mountainous regions of varying catchment scales that are smaller than the typical spatial scale of general circulation models.

It should be noted that the long-term simulations presented here are based on changes in climate alone, and they do not consider possible changes in land use, biodiversity, demographics, regulations and technological advances whose feedback on climate may alter the results of the scenarios examined here. The results presented here describe likely scenarios under two opposite spectrums of climate change. Consideration of the land-use and land-cover changes, climate mitigation and adaptation strategies, as well as improvement in the model processes and projections will help reduce the uncertainties in the projected changes in snow dynamics in mountainous regions.

CRediT authorship contribution statement

Santosh Nepal: Conceptualization, Methodology, Software, Formal analysis, Data curation, Writing – original draft, Writing – review & editing, Visualization. **Kabi Raj Khatiwada:** Conceptualization, Methodology, Formal analysis, Data curation, Writing – review & editing, Visualization. **Saurav Pradhananga:** Conceptualization, Methodology, Formal analysis, Data curation, Writing – review & editing, Visualization. **Sven Kralisch:** Conceptualization, Methodology, Software, Formal analysis, Data curation, Writing – review & editing, Visualization, Project administration. **Denis Samyn:** Conceptualization, Methodology, Writing – review & editing. **Mohammad Tayib Bromand:** Conceptualization, Methodology, Writing – review & editing. **Najeebullah Jamal:** Conceptualization, Methodology, Writing – review & editing. **Milad Dildar:** Conceptualization, Methodology, Writing – review & editing. **Fazlullah Durrani:** Conceptualization, Methodology, Writing – review & editing. **Farangis Rassouly:** Conceptualization, Methodology, Writing – review & editing. **Fayezurahman Azizi:** Conceptualization, Methodology, Writing – review & editing. **Wahidullah Salehi:** Conceptualization, Methodology, Writing – review & editing. **Rohullah Malikzooi:** Conceptualization, Methodology, Writing – review & editing. **Peter Krause:** Conceptualization, Methodology, Writing – review & editing. **Sujan Koirala:** Conceptualization, Methodology, Writing – review & editing. **Pierre Chevallier:** Conceptualization, Methodology, Writing – review & editing.

Declaration of competing interest

The authors declare that they have no known competing financial interests or personal relationships that could have appeared to influence the work reported in this paper.

Acknowledgements

Appendix A. Supplementary data

Supplementary data to this article can be found online at https://doi.org/10.1016/j.scitotenv.2021.148587.

References

Archer, D.R., Fowler, H.J., 2004. Spatial and temporal variations in precipitation in the Upper Indus Basin, global teleconnections and hydrological implications. Hydrol. Earth Syst. Sci. 8, 47–61.

Armstrong, R.L., Rittger, K., Brodzik, M.J., Racoviteanu, A., Barrett, A.P., Khalsa, S.-J.S., Raup, B., Hill, A.F., Khan, A.L., Wilson, A.M., Kayastha, R.B., Fetterer, F., Armstrong, B., 2019. Runoff from glacier ice and seasonal snow in High Asia: separating melt water sources in river flow. Reg. Environ. Chang. 19, 1249–1261. https://doi.org/10.1007/s10113-018-1429-0.

Azizi, A.H., Asaoka, Y., 2020. Assessment of the impact of climate change on snow distribution and river flows in a snow-dominated mountainous watershed in the Western Hindukush–Himalaya, Afghanistan. Hydrology 7, 74. https://doi.org/10.3390/hydrology7040074.

Barnett, T.P., Adam, J.C., Lettenmaier, D.P., 2005. Potential impacts of a warming climate on water availability in snow-dominated regions. Nature 438, 303–309. https://doi.org/10.1038/nature04141.

Beven, K., Binley, A., 1992. The future of distributed models: model calibration and uncertainty prediction. Hydrol. Process. 6, 279–298. https://doi.org/10.1002/hyp.3360060305.

Bhatta, B., Shrestha, S., Shrestha, P.K., Talchabhadel, R., 2020. Modelling the impact of past and future climate scenarios on streamflow in a highly mountainous watershed: a case study in the West Seti River Basin, Nepal. Sci. Total Environ. 740, 140156. https://doi.org/10.1016/j.scitotenv.2020.140156.

Bhutiyani, M., Kale, V., Pawar, N., 2007. Long-term trends in maximum, minimum and mean annual air temperatures across the Northwestern Himalaya during the twentieth century. Clim. Chang. 85, 159–177.

Biemans, H., Siderius, C., Lutz, A.F., Nepal, S., Ahmad, B., Hassan, T., von Bloh, W., Wijngaard, R.R., Wester, P., Shrestha, A.B., Immerzeel, W.W., 2019. Importance of snow and glacier meltwater for agriculture on the Indo-Gangetic Plain. Nat. Sustain. 2, 594–601. https://doi.org/10.1038/s41893-019-0305-3.

Bolch, T., Kulkarni, a., Kaab, A., Huggel, C., Paul, F., Cogley, J.G., Frey, H., Kargel, J.S., Fujita, K., Scheel, M., Bajracharya, S., Stoffel, M., 2012. The state and fate of Himalayan glaciers. Science 336, 310–314. https://doi.org/10.1126/science.1215828.

Bolch, T., Shea, J.M., Liu, S., Azam, F.M., Gao, Y., Gruber, S., Immerzeel, W.W., Kulkarni, A., Li, H, Tahir, A.A., Zhang, G., Zhang, Y., 2019. Status and change of the cryosphere in the extended Hindu Kush Himalaya Region. The Hindu Kush Himalaya Assessment https://doi.org/10.1007/978-3-319-92288-1_7.

Bormann, K.J., Brown, R.D., Derksen, C., Painter, T.H., 2018. Estimating snow-cover trends from space. Nat. Clim. Chang. 8, 924. https://doi.org/10.1038/s41558-018-0318-3.

Bouchard, B., Eeckman, J., Dedieu, J.P., Delclaux, F., Chevallier, P., Gascoin, S., Arnaud, Y., 2019. On the interest of optical remote sensing for seasonal snowmelt parameterization, applied to the Everest Region (Nepal). Remote Sens. 11. https://doi.org/10.3390/rs11222598.

Castebrunet, H., Eckert, N., Giraud, G., Durand, Y., Morin, S., 2014. Projected changes of snow conditions and avalanche activity in a warming climate: the French Alps over the 2020–2050 and 2070–2100 periods. Cryosph 8, 1673–1697. https://doi.org/10.5194/tc-8-1673-2014.

Chevallier, P., Pouyaud, B., Mojaïsky, M., Bolgov, M., Olsson, O., Bauer, M., Froebrich, J., 2014. River flow regime and snow cover of the Pamir Alay (Central Asia) in a changing climate. Hydrol. Sci. J. https://doi.org/10.1080/02626667.2013.838004.

Cordero, R.R., Asencio, V., Feron, S., Damiani, A., Llanillo, P.J., Sepulveda, E., Jorquera, J., Carrasco, J., Casassa, G., 2019. Dry-season snow cover losses in the Andes (18°–40°S) driven by changes in large-scale climate modes. Sci. Rep. 9, 1–10. https://doi.org/10.1038/s41598-019-53486-7.

Dahri, Z.H., Ludwig, F., Moors, E., Ahmad, Shakil, Ahmad, B., Ahmad, Sarfraz, Riaz, M., Kabat, P., 2021. Climate change and hydrological regime of the high-altitude Indus basin under extreme climate scenarios. Sci. Total Environ. 768, 144467. https://doi.org/10.1016/j.scitotenv.2020.144467.

Defourny, P., Vancutsem, C., Bicheron, C., Brockmann, C., Nino, F., Schouten, L., Leroy, M., 2006. GLOBCOVER : A 300 M Global Land Cover Product for 2005 Using ENVISAT MERIS Time Series. ISPRS Commission VII Mid-term Symposium "Remote Sensing: From Pixels to Processes", Enschede, the Netherlands, 8–11 May 2006.

Eeckman, J., Nepal, S., Chevallier, P., Camensuli, G., Delclaux, F., Boone, A., De Rouw, A., 2019. Comparing the ISBA and J2000 approaches for surface flows modelling at the local scale in the Everest region. J. Hydrol. 569, 705–719. https://doi.org/10.1016/j.jhydrol.2018.12.022.

FAO/IIASA/ISRIC/ISS-CAS/JRC, 2012. Harmonized world soil database, version 1.2. Laxenburg, Austria. Data available at:. http://www.fao.org/soils-portal/data-hub/soil-maps-and-databases/harmonized-world-soil-database-v12/en/.

Fowler, H.J., Archer, D.R., 2006. Conflicting signals of climatic change in the Upper Indus Basin. J. Clim. 19, 4276–4293.

Gaddam, V.K., Kulkarni, A.V., Gupta, A.K., 2018. Assessment of snow-glacier melt and rainfall contribution to stream runoff in Baspa Basin, Indian Himalaya. Environ. Monit. Assess. 190, 1–11. https://doi.org/10.1007/s10661-018-6520-y.

Gentle, P., Maraseni, T.N., 2012. Climate change, poverty and livelihoods: adaptation practices by rural mountain communities in Nepal. Environ. Sci. Pol. 21, 24–34. https://doi.org/10.1016/j.envsci.2012.03.007.

Gurung, D.R., Amarnath, G., Khun, S.A., Shrestha, B., A.V., K., 2011. Snow-cover Mapping and Monitoring in the Hindu Kush-Himalayas. ICIMOD, Kathmandu.

Hall, D.K., Riggs, G.A., 2007. Accuracy assessment of the MODIS snow products. Hydrol. Process. https://doi.org/10.1002/hyp.6715.

Hersbach, H., Bell, B., Berrisford, P., Hirahara, S., Horányi, A., Muñoz-Sabater, J., Nicolas, J., Peubey, C., Radu, R., Schepers, D., Simmons, A., Soci, C., Abdalla, S., Abellan, X., Balsamo, G., Bechtold, P., Biavati, G., Bidlot, J., Bonavita, M., De Chiara, G., Dahlgren, P., Dee, D., Diamantakis, M., Dragani, R., Flemming, J., Forbes, R., Fuentes, M., Geer, A., Haimberger, L., Healy, S., Hogan, R.J., Hólm, E., Janisková, M., Keeley, S., Laloyaux, P., Lopez, P., Lupu, C., Radnoti, G., de Rosnay, P., Rozum, I., Vamborg, F., Villaume, S., Thépaut, J.N., 2020. The ERA5 global reanalysis. Q. J. R. Meteorol. Soc. https://doi.org/10.1002/qj.3803.

Hock, R., Rasul, G., Adler, C., Cáceres, B., Gruber, S., Hirabayashi, Y., Jackson, M., Kääb, A., Kang, S., Kutuzov, S., Milner, A., Molau, U., Morin, S., Orlove, B., Steltzer, H.I., 2019. Chapter 2: high mountain areas. IPCC special report on the ocean and cryosphere in a changing climate. In: Pörtner, H.-O., Roberts, D.C., Masson-Delmotte, V., Zhai, P., Tignor, M., Poloczanska, E., Mintenbeck, K., Alegría, A., Nicolai, M., Okem, A., Petzold, J., Rama, B., Weyer, N.M. (Eds.), IPCC Special Report on the Ocean and Cryosphere in a Changing Climate, pp. 131–202 In Press.

Immerzeel, W.W., Pellicciotti, F., Bierkens, M.F.P., 2013. Rising river flows throughout the twenty-first century in two Himalayan glacierized watersheds. Nat. Geosci. https://doi.org/10.1038/ngeo1896.

Immerzeel, W.W., Wanders, N., Lutz, A.F., Shea, J.M., Bierkens, M.F.P., 2015. Reconciling high-altitude precipitation in the upper Indus basin with glacier mass balances and runoff. Hydrol. Earth Syst. Sci. 19, 4673–4687. https://doi.org/10.5194/hess-19-4673-2015.

Immerzeel, W.W., Lutz, A.F., Andrade, M., et al., 2020. Importance and vulnerability of the world's water towers. Nature 577, 364–369. https://doi.org/10.1038/s41586-019-1822-y.

Ingty, T., 2017. High mountain communities and climate change: adaptation, traditional ecological knowledge, and institutions. Clim. Chang. 145, 41–55. https://doi.org/10.1007/s10584-017-2080-3.

Jeelani, G., Feddema, J.J., van der Veen, C.J., Stearns, L., 2012. Role of snow and glacier melt in controlling river hydrology in Liddar watershed (western Himalaya) under current and future climate. Water Resour. Res. 48. https://doi.org/10.1029/2011WR011590.

Kaini, S., Nepal, S., Pradhananga, S., Gardner, T., Sharma, A.K., 2020. Representative general circulation models selection and downscaling of climate data for the transboundary Koshi river basin in China and Nepal. Int. J. Climatol. 40, 4131–4149. https://doi.org/10.1002/joc.6447.

Kendall, M.G., 1975. Rank Correlation Methods. Charles Griffin, London.

Khadka, N., Khadka, N., Ghimire, S.K., Chen, X., Thakuri, S., Hamal, K., Shrestha, D., Sharma, S., 2020. Dynamics of maximum snow cover area and snow line altitude across Nepal (2003-2018) using improved MODIS data. J. Instr. Sci. Technol. 25. https://doi.org/10.3126/jist.v25i2.33729.

Khattak, M.S.S., Babel, M.S.S., Sharif, M., 2011. Hydro-meteorological trends in the upper Indus River basin in Pakistan. Clim. Res. 46, 103–119.

Knauf, D., 1980. Die Berechnung des Abflüsses aus einer Schneedecke. Analyse und Berechnung oberirdischer Abflüsse DVWK- Schriften, Bonn, Heft. p. 46.

Kraaijenbrink, P.D.A., Bierkens, M.F.P., Lutz, A.F., Immerzeel, W.W., 2017. Impact of a global temperature rise of 1.5 degrees Celsius on Asia's glaciers. Nature https://doi.org/10.1038/nature23878.

Krause, P., 2001. Das hydrologische Modellsystem J2000: Beschreibung und Anwendung in großen Flußeinzugsgebieten. Schriften des Forschungszentrum Jülich. Reihe Umwelt/Environment, Band, p. 29.

Krause, P., 2002. Quantifying the impact of land use changes on the water balance of large catchments using the J2000 model. Phys. Chem. Earth 27 (9), 663–673.

Kripalani, R.H., Kulkarni, A., Sabade, S.S., 2003. Western Himalayan snow cover and Indian monsoon rainfall: a re-examination with INSAT and NCEP/NCAR data. Theor. Appl. Climatol. 74. https://doi.org/10.1007/s00704-002-0699-z.

Kripalani, R.H., Oh, J.H., Kulkarni, A., Sabade, S.S., Chaudhari, H.S., 2007. South Asian summer monsoon precipitation variability: coupled climate model simulations and projections under IPCC AR4. Theor. Appl. Climatol. 90, 133–159. https://doi.org/10.1007/s00704-006-0282-0.

Li, H., Haugen, J.E., Xu, C.Y., 2018. Precipitation pattern in the Western Himalayas revealed by four datasets. Hydrol. Earth Syst. Sci. https://doi.org/10.5194/hess-22-5097-2018.

Lutz, A.F., Immerzeel, W.W., Shrestha, A.B., Bierkens, M.F.P.P., 2014. Consistent increase in High Asia's runoff due to increasing glacier melt and precipitation. Nat. Clim. Chang. 4, 587–592. https://doi.org/10.1038/nclimate2237.

Lutz, A.F., ter Maat, H.W., Biemans, H., Shrestha, A.B., Wester, P., Immerzeel, W.W., 2016. Selecting representative climate models for climate change impact studies: an advanced envelope-based selection approach. Int. J. Climatol. 36, 3988–4005.

Mann, H.B., 1945. Non-parametric test against trend. Econometrica 13.

Marty, C., Tilg, A.-M., Jonas, T., 2017. Recent evidence of large-scale receding snow water equivalents in the European Alps. J. Hydrometeorol. 18, 1021–1031. https://doi.org/10.1175/JHM-D-16-0188.1.

Maskey, S., Uhlenbrook, S., Ojha, S., 2011. An analysis of snow cover changes in the Himalayan region using MODIS snow products and in-situ temperature data. Clim. Chang. https://doi.org/10.1007/s10584-011-0181-y.

Ménégoz, M., Krinner, G., Balkanski, Y., Cozic, A., Boucher, O., Ciais, P., 2013. Boreal and temperate snow cover variations induced by black carbon emissions in the middle of the 21st century. Cryosph 7, 537–554. https://doi.org/10.5194/tc-7-537-2013.

Mimeau, L., Esteves, M., Zin, I., Jacobi, H.W., Brun, F., Wagnon, P., Koirala, D., Arnaud, Y., 2019. Quantification of different flow components in a high-altitude glacierized catchment (Dudh Koshi, Himalaya): some cryospheric-related issues. Hydrol. Earth Syst. Sci., 23 https://doi.org/10.5194/hess-23-3969-2019.

Muhammad, S., Thapa, A., 2020. An improved Terra–Aqua MODIS snow cover and Randolph Glacier Inventory 6.0 combined product (MOYDGL06*) for high-mountain Asia between 2002 and 2018. Earth Syst. Sci. Data 12, 345–356. https://doi.org/10.5194/essd-12-345-2020.

Muhammad, S., Thapa, A., 2021. Daily Terra-Aqua MODIS cloud-free snow and Randolph Glacier Inventory 6.0 combined product (M*D10A1GL06) for high-mountain Asia between 2002 and 2019. Earth Syst. Sci. Data 13, 767–776. https://doi.org/10.5194/essd-13-767-2021.

Muñoz-Sabater, J., Dutra, E., Agustí-Panareda, A., Albergel, C., Arduini, G., Balsamo, G., Boussetta, S., Choulga, M., Harrigan, S., Hersbach, H., 2021. ESSDD - ERA5-Land: a state-of-the-art global reanalysis dataset for land applications [WWW Document]. Earth Syst. Sci. Data Discuss. https://doi.org/10.5194/essd-2021-82 URL. https://essd.copernicus.org/preprints/essd-2021-82/ (accessed 5.20.21).

Nepal, S., Shrestha, A.B., 2015. Impact of climate change on the hydrological regime of the Indus, Ganges and Brahmaputra river basins: a review of the literature. Int. J. Water Resour. Dev. 31, 201–218. https://doi.org/10.1080/07900627.2015.1030494.

Nepal, S., Krause, P., Flügel, W.-A., Fink, M., Fischer, C., 2014. Understanding the hydrological system dynamics of a glaciated alpine catchment in the Himalayan region using the J2000 hydrological model. Hydrol. Process. 28, 1329–1344.

Nepal, S., Flügel, W.A., Krause, P., Fink, M., Fischer, C., 2017. Assessment of spatial transfer-ability of process-based hydrological model parameters in two neighbouring catchments in the Himalayan Region. Hydrol. Process. 31, 2812–2826. https://doi.org/10.1002/hyp.11199.

Nepal, S., Pandey, A., Shrestha, A., Mukherji, A., 2018. Revisiting Key Questions Regarding Upstream-Downstream Linkages of Land and Water Management in the Hindu Kush Himalaya (HKH) Region. ICIMOD, Kathmandu.

Nepal, S., Khatiwada, K.R., Pradhananga, S., Kralisch, S., 2020. Application of the J2000 Hydrological Model in the Panjshir Catchment of the Hindu Kush Himalayan Region, Training Manual. ICIMOD, Kathmandu.

Nepal, S., Pradhananga, S., Shrestha, N.K., Kralisch, S., Shrestha, J., Fink, M., 2021. Space-time variability of soil moisture droughts in the Himalayan region. Hydrol. Earth Syst. Sci. 25, 1761–1783. https://doi.org/10.5194/hess-2020-337.

Nie, Y., Pritchard, H.D., Liu, Q., Hennig, T., Wang, W., Wang, X., Liu, S., Nepal, S., Samyn, D., Hewitt, K., Chen, X., 2021. Glacial change and hydrological implications in the Himalaya and Karakoram. Nat. Rev. Earth Environ., 1–16 https://doi.org/10.1038/s43017-020-00124-w.

Qin, D.H., Liu, S.Y., Li, P.J., 2006. Snow cover distribution, variability, and response to climate change in western China. J. Clim. 19, 1820–1833. https://doi.org/10.1175/jcli3694.1.

Qureshi, A.S., 2002. Water Resources Management in Afghanistan: The Issues and Options. vol. 49 (Colombo).

Rasul, G., Kazmi, D.H., 2011. Climate change and challenges to crop production. Proceedings of International Workshop on Plant Conservation & Reversing Desertification. A Way Forward. PMAS Arid Agriculture University, Rawalpindi, pp. 81–99.

Scott, C.A., Zhang, F., Mukherji, A., Immerzeel, W., Mustafa, D., Bharati, L., 2019. Water in the Hindu Kush Himalaya. The Hindu Kush Himalaya Assessment. Springer International Publishing, pp. 257–299 https://doi.org/10.1007/978-3-319-92288-1_8.

Sen, P.K., 1968. Estimates of the regression coefficient based on Kendall's Tau. J. Am. Stat. Assoc. 63 (324), 1379–1389.

Shahid, M., Rahman, K.U., 2021. Identifying the annual and seasonal trends of hydrological and climatic variables in the Indus Basin Pakistan. Asia-Pacific J. Atmos. Sci. 57, 191–205. https://doi.org/10.1007/s13143-020-00194-2.

Sharma, E., Molden, D., Rahman, A., Khatiwada, Y.R., Zhang, L., Singh, S.P., Yao, T., Wester, P., 2019. Introduction to the Hindu Kush Himalaya assessment. The Hindu Kush Himalaya Assessment https://doi.org/10.1007/978-3-319-92288-1_1.

Shen, Y.J., Shen, Y.J., Fink, M., Kralisch, S., Chen, Y.N., Brenning, A., 2018. Trends and variability in streamflow and snowmelt runoff timing in the southern Tianshan Mountains. J. Hydrol. 557, 173–181. https://doi.org/10.1016/j.jhydrol.2017.12.035.

Shrestha, S., Nepal, S., 2019. Water balance assessment under different glacier coverage scenarios in the Hunza basin. Water, 11 https://doi.org/10.3390/w11061124.

Singh, S.K., Rathore, B.P., Bahuguna, I.M., Ajai, 2014. Snow cover variability in the Himalayan-Tibetan region. Int. J. Climatol. https://doi.org/10.1002/joc.3697.

Tahir, A.A., Chevallier, P., Arnaud, Y., Ahmad, B., 2011. Snow cover dynamics and hydrological regime of the Hunza River basin, Karakoram Range, Northern Pakistan. Hydrol. Earth Syst. Sci. 15, 2275–2290. https://doi.org/10.5194/hess-15-2275-2011.

Taylor, K.E., Stouffer, R.J., Meehl, G.A., 2012. An overview of CMIP5 and the experiment design. Bull. Am. Meteorol. Soc. https://doi.org/10.1175/BAMS-D-11-00094.1.

Terzago, S., von Hardenberg, J., Palazzi, E., Provenzale, A., 2014a. Snowpack changes in the Hindu Kush-Karakoram-Himalaya from CMIP5 global climate models. J. Hydrometeorol. https://doi.org/10.1175/JHM-D-13-0196.1.

Terzago, S., von Hardenberg, J., Palazzi, E., Provenzale, A., Terzago, S., von Hardenberg, J., Palazzi, E., Provenzale, A., 2014b. Snowpack changes in the Hindu Kush–Karakoram–Himalaya from CMIP5 global climate models. J. Hydrometeorol. 15, 2293–2313. https://doi.org/10.1175/JHM-D-13-0196.1.

Themeßl, M.J., Gobiet, A., Heinrich, G., 2011. Empirical-statistical downscaling and error correction of regional climate models and its impact on the climate change signal. Clim. Chang. 112, 449–468. https://doi.org/10.1007/s10584-011-0224-4.

Viste, E., Sorteberg, A., 2015. Snowfall in the Himalayas: an uncertain future from a little-known past. Cryosphere https://doi.org/10.5194/tc-9-1147-2015.

Viviroli, D., Kummu, M., Meybeck, M., Kallio, M., Wada, Y., 2020. Increasing dependence of lowland populations on mountain water resources. Nat. Sustain. 3, 917–928. https://doi.org/10.1038/s41893-020-0559-9.

Wijngaard, R.R.R., Lutz, A.F.F., Nepal, S., Khanal, S., Pradhananga, S., Shrestha, A.B.B., Immerzeel, W.W.W., 2017. Future changes in hydro-climatic extremes in the Upper Indus, Ganges, and Brahmaputra River basins. PLoS One 12, 1–26. https://doi.org/10.1371/journal.pone.0190224.

Zaman, Q., Khan, S.N., 2020. The application of Geographic Information System (GIS) and remote sensing in quantifying snow cover and precipitation in Kabul Basin. Geosfera Indones 5, 80. https://doi.org/10.19184/geosi.v5i1.14896.